Title: Correlated Electronic States in Conjugated Polymers: A DMRG Approach

Date: May 18, 2012 02:30 PM

URL: http://pirsa.org/12050051

Abstract: Electrons in conjugated organic polymers and molecules are strongly correlated since most of these systems are quasi one-dimensional. Experimental evidences include existence of two photons below one photon state, observation of negative spin densities in polyene radicals and qualitatively different behavior of optical gaps in polyenes and closely related symmetric cynanine dyes in the thermodynamic limiy. In this talk, I will introduce the model Hamiltonians for the electron states in conjugated systems. The DMRG method is ideally suited for their study. Modifications to the DMRG method to obtain important low-lying states of the systems and methods of obtaining linear and nonlinear optical response coefficients using the DMRG technique will be discussed [1-4]. Application of the method to the study of a wide variety of conjugated systems will be touched upon [5,7]. I will also discuss some recent applications of wave-packet dynamics in the study of some time-dependent phenomena [8]. References [1] S. Ramasesha, Swapan K Pati, H.R. Krishnamurthy, Z. Shuai and J. L. BrÂ´edas, (1996) â€œSymmetrized DMRG method for the excited states of Hubbard modelsâ€•, Phys. Rev. B 54, 7598. [2] Z. Shuai, J. L. BrÂ´edas, Swapan K. Pati and S. Ramasesha, (1998) â€œComment on the exciton binding energy in the strong correlation limit of conjugated chainsâ€•, Phys. Rev. B 58, 15329. [3] Z. Shuai, J. L. BrÂ´edas, Swapan K. Pati and S. Ramasesha, (1997) â€œQuantum conï¬•nement eï¬€ects on the ordering of the lowest-lying excited states in conjugated chainsâ€•, Phys. Rev. B 56, 9298. [4] Swapan K Pati, S. Ramasesha, Z. Shuai and J. L. BrÂ´edas, (1999) â€œDynamic nonlinear optical properties from the symmetrized density matrix renormalization group methodâ€•, Phys. Rev. B 59, 14827. [5] C. Raghu, Y. Anusooya Pati and S. Ramasesha, (2002) â€œA density matrix renormalization group study of low-lying excitations of polyacene within a Pariser-Parr-Pople modelâ€•, Phys. Rev. B 66, 035116. [6] S. Mukhopadhyay and S. Ramasesha (2009) â€œStudy of linear and nonlinear optical properties of dendrimers using density matrix renormalization group methodâ€•, J. Chem. Phys. 131, 074111. [7] M. Kumar and S. Ramasesha, (2010) â€œA DMRG Study of the Low-Lying States of Transverse Substituted Trans-polyacetylene and Trans-polyacetyleneâ€•, Phys. Rev. B. 81, 035115 [8] Tirthankar Dutta and S. Ramasesha, (2010) â€œDouble time window targeting technique: Real-time DMRG dynamics in Pariser-Parr-Pople modelâ€•, Phys. Rev. B 82, 035115. [9] Simil Thomas, Daniel Garcia, Karen Hallberg and S. Ramasesha "Fused Azulenes: Possible Organic Multiferroics", Phys. Rev. B RC (communicated)

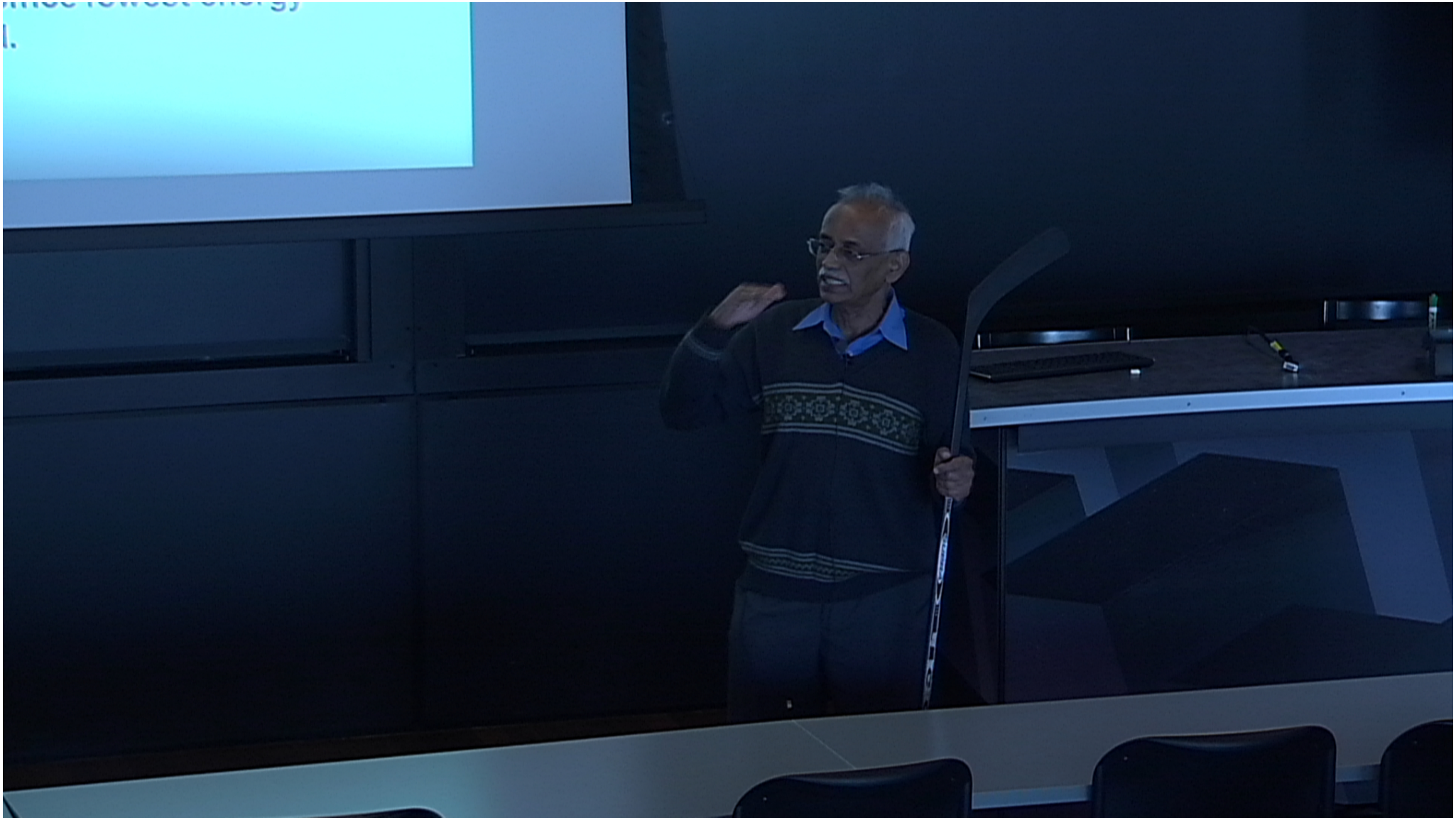

Correlated Electronic States in Conjugated Polymers: A DMRG Approach

S. Ramasesha
ramasesh@sscu.iisc.ernet.in
Solid State and Structural Chemistry Unit
Indian Institute of Science, Bangalore 560 012, India

Collaborators:

Anusooya Pati
C. Raghu
Sukrit Mukhopadhyay
Tirthankar Dutta
H.R. Krishnamurthy
Swapan Pati
Manoranjan Kumar
Simil Thomas
Diptiman Sen

Funding: DST, India; CSIR, India; BRNS, India

Perimeter Institute for Theoretical Physics
Waterloo, Canada, May 18, 2012


India
भारत
State or Union Territory
National Capital
State or Union Territory Capital
© Nations Online Project
Turkmenistan
Uzbek
Tajikistan
Afghanistan
Kabul
Islamabad
Pakistan
Pakistani line of control
Chinese line of control
Jammu & Kashmir
Srinagar
Jammu
China
Himachal Pradesh
Shimla
Punjab
Chandigarh
Dehra Dun
Uttaranchal
Haryana
New Delhi
Delhi
Nepal
Kathmandu
Tibet
Sikkim
Gangtok
Bhutan
Thimphu
Itanagar
Arunachal Pradesh
Assam
Dispur
Nagaland
Kohima
Shillong
Meghalaya
Manipur
Imphal
Agartala
Tripura
Aizawl
Mizoram
Bangladesh
Dhaka
Myanmar
Rangoon
Jaipur
Rajasthan
Lucknow
Uttar Pradesh
Patna
Bihar
Jharkhand
Ranchi
West Bengal
Kolkata (Calcutta)
Gandhinagar
Gujarat
Bhopal
Madhya Pradesh
Chhattis-garh
Raipur
Orissa
Bhubaneswar
Daman
Diu
Dadra & Nagar Haveli
Daman
Silvassa
Maharashtra
Mumbai (Bombay)
Hyderabad
Andhra Pradesh
Pondicherry
Arabian Sea
Bay of Bengal
Panaji
Goa
Karnataka
Bangalore
Chennai (Madras)
Pondicherry
Pondicherry
Tamil Nadu
Pondicherry
Kavaratti
Lakshadweep
Kerala
Thiruvananthapuram
Andaman Islands
Port Blair
Andaman and Nicobar Islands
Andaman Sea
Nicobar Islands
Sri Lanka
Colombo
Laccadive Sea
Maldives
Indian Ocean
0 200 400 Kilometers
0 200 400 Miles

Bangalore

2

Indian Institute of Science, Bangalore

3

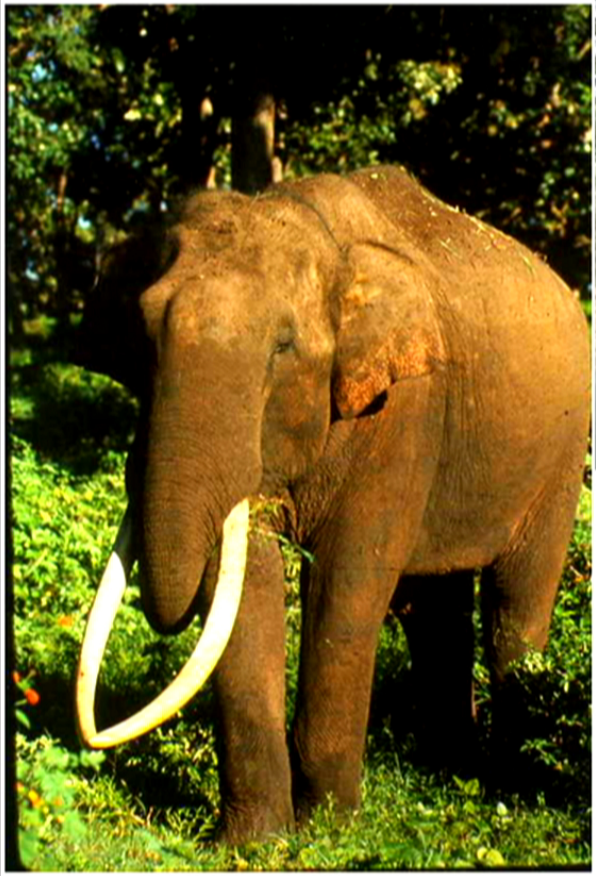

Plan of the Talk

1. Introduction to conjugated systems
2. Noninteracting model and its limitations
3. Introduction to interacting model
4. The DMRG method for excited states
5. Some applications
6. Dynamic DMRG method
7. Summary

Conjugated Electronic Materials

Organic molecules with extended π - conjugation

Examples – polymers and large molecules

Poly Acetylene (PA), Poly Para Phenylene Vinylene (PPV)

Oligo thiophenes, Oligo acenes, Porphines, Pthalocyanines . . .

Applications:

Organic Light Emitting Diodes (OLEDs)

Organic Photovoltaics (OPVs)

Organic Transistors (OTFTs, OFETs)

Examples of Conjugated Polymers

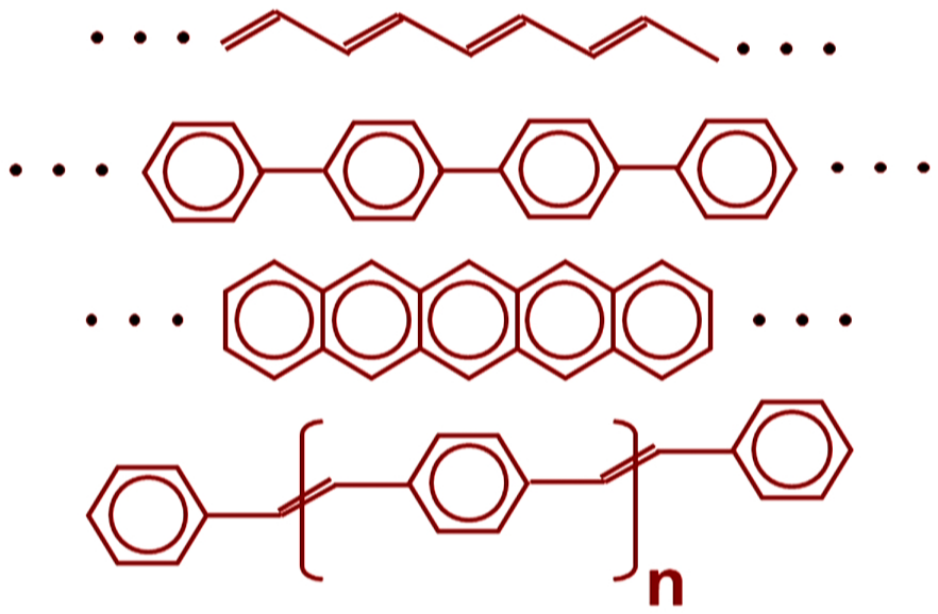

From top: Poly acetylene $(CH)_x$, poly para phenylene (PPP)
poly acene and poly para phenylene vinylene (PPV)

Theoretical Models for π-Conjugated Systems

Hückel Model:

Carbon atoms are in sp^2 hybridization.

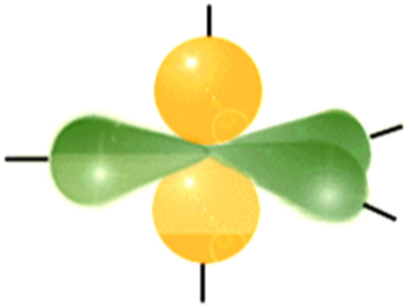

Assumes one p_z orbital at every Carbon site involved in conjugation.

Assumes transfer integral only between bonded Carbon sites.

$$\hat{H}_o = \sum_{<ij>} t_{ij} \left(\hat{a}^{\dagger}_{i\sigma} \hat{a}_{j\sigma} + H.c.\right) + \sum_i \alpha_i \hat{n}_i$$

t_{ij} is resonance / transfer integral between bonded sites and α_i, the site energy at site '*i*'.

$(CH)_x$ and Symmetries in the MO picture

- $(CH)_x$ has charge conjugation or electron-hole or alternancy symmetry. Carbon sites when subdivided into two sublattices, no bond exists between carbon atoms on same sublattice.

$$C^A=C^B\,C^A=C^B\,C^A=C^B\,C^A=C^B$$

- The polymer also has inversion symmetry.
- Weak spin-orbit interactions; states can be classified by total spin.
- Symmetries lead to strong experimental predictions.

$(CH)_x$ and Symmetries in the MO picture

- $(CH)_x$ has charge conjugation or electron-hole or alternancy symmetry. Carbon sites when subdivided into two sublattices, no bond exists between carbon atoms on same sublattice.

$$C^A=C^B\,C^A=C^B\,C^A=C^B\,C^A=C^B$$

- The polymer also has inversion symmetry.
- Weak spin-orbit interactions; states can be classified by total spin.
- Symmetries lead to strong experimental predictions.

Consequences of Symmetry

- Pairing theorem follows from alternancy symmetry predicts that for a π bonding state at energy $-\varepsilon_k$, there exists a π^* anti-bonding state at $+\varepsilon_k$.
- Symmetry of states alternate between a^+ and b^-, so lowest energy excitation is dipole allowed.
- Pairing theorem implies, $(CH)_x$ with odd number of carbon atoms should have a mid-gap state. and a mid-gap absorption since lowest energy excitation is dipole allowed.

Schematic MO Picture of Even and Odd Polyenes

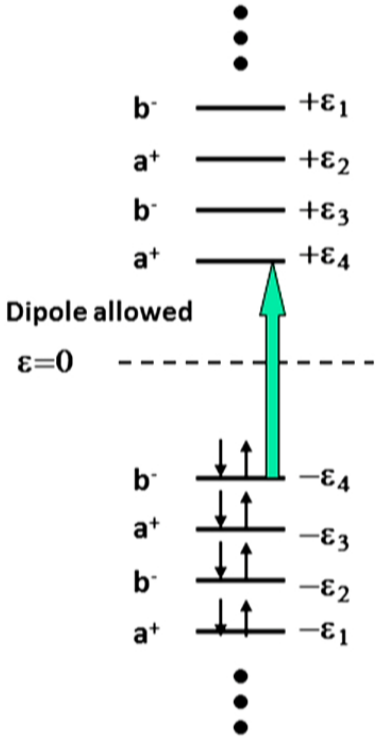

Even polyene

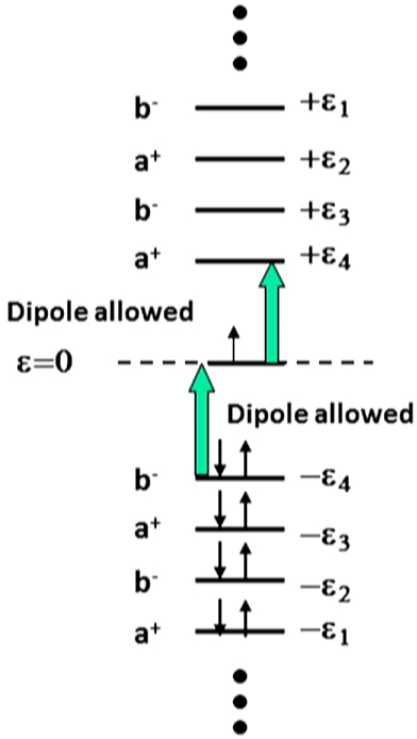

Odd polyene

Polymer or Band Limit

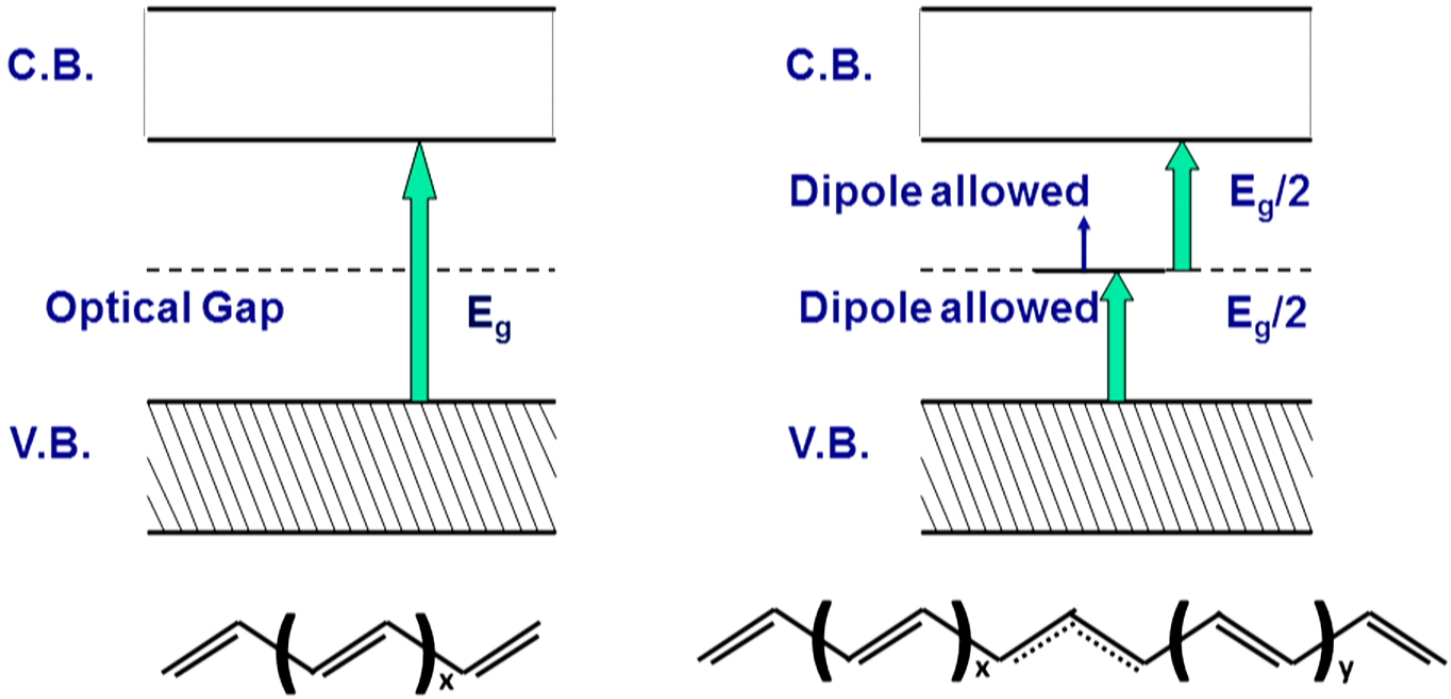

The kink in odd polyene is a topological soliton and is associated with a mid gap state.

12

Experimental Status

- Polyacetylene is a semiconductor due to Peierls' distortion. Valence π band is filled and conduction π^* band is empty.
- The optical gap ~ 1.7eV. Dimerization required to obtain this gap twice the observed bond length alternation.
- Evidence for dipole forbidden states below E_g.
- No evidence for mid-gap absorption in polyene radicals.
- *esr* studies of polyene radicals show evidence for both positive and negative spin densities.

Symmetric Cyanine Dyes: An intrigue

SCD = 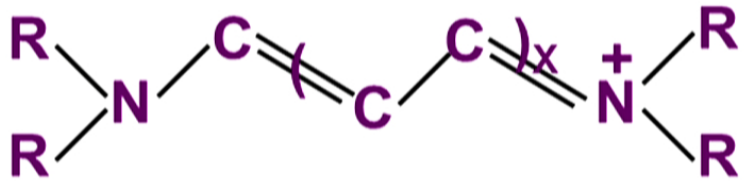

SCD similar to $(CH)_x$ except for end groups.

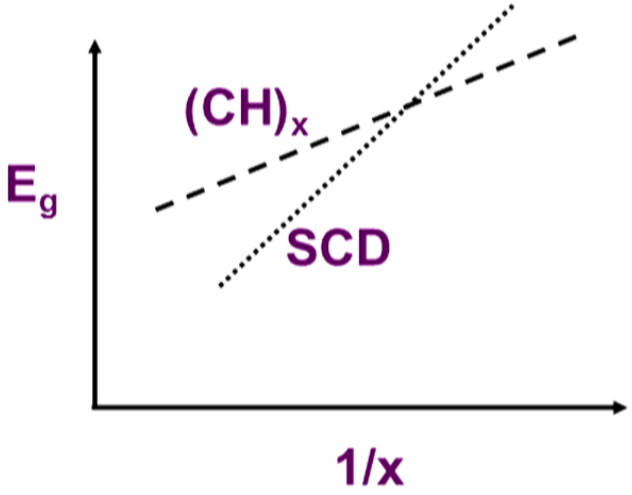

Qualitatively different E_g vs 1/x extrapolation in $(CH)_x$ and SCD.

E_g for Infinite chains in $(CH)_x$ is nonzero, but in SCD it is zero.

Hückel model for molecules → Single band tight – binding model in Solids

Drawbacks of Hückel model:

- Gives incorrect ordering of energy levels in polyenes.
- Fails to account for negative spin densities in radicals and yields wrong spin-spin correlations.
- Fails to reproduce qualitative differences between closely related systems.
- Mainly of pedagogical value. Ignores explicit electron-electron interactions.

Interacting π–Electron Models

- Explicit electron – electron interactions essential for realistic modeling

$$\hat{H}_{Full} = \hat{H}_o + \tfrac{1}{2} \sum_{ijkl} [ij|kl] \, (\hat{E}_{ij}\hat{E}_{kl} - \delta_{jk}\hat{E}_{il})$$

$$\hat{E}_{ij} = \sum_{\sigma} \hat{a}^{\dagger}_{i,\sigma}\hat{a}_{j,\sigma}$$

$$[ij|kl] = \int \phi_i^*(1)\, \phi_j(1)\, (e^2/r_{12})\, \phi_k^*(2)\, \phi_l(2)\, d^3r_1 d^3r_2$$

This model requires further simplification to enable routine solvability.

Zero Differential Overlap (*ZDO*) Approximation

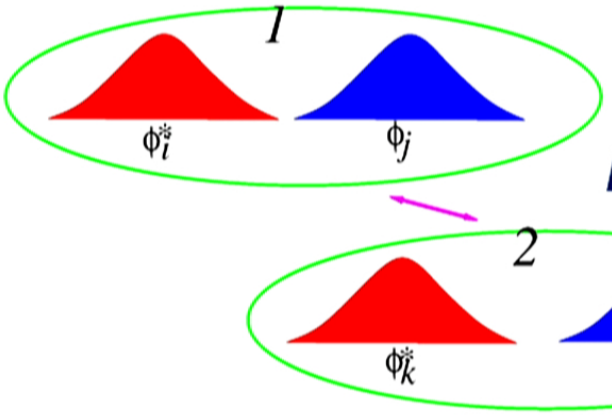

$$[ij|kl] = \int \phi_i^*(1)\, \phi_j(1)\, (e^2/r_{12})\, \phi_k^*(2)\, \phi_l(2)\, d^3r_1 d^3r_2$$

$$[ij|kl] = [ij|kl]\delta_{ij}\,\delta_{kl}$$

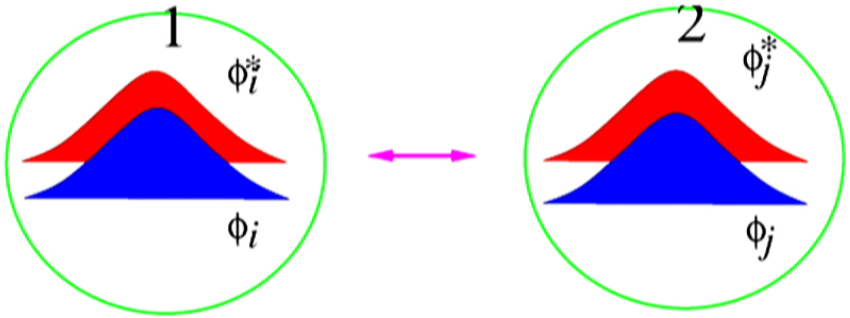

Pariser-Parr-Pople (PPP) Model

[ii|jj] parametrized by $V(r_{ij})$

$$\hat{H}_{PPP} = \hat{H}_{Hub} + \sum_{i>j} V(r_{ij}) (\hat{n}_i - z_i) (\hat{n}_j - z_j)$$

z_i are local chemical potentials.

- Ohno parametrization:

$$V(r_{ij}) = \{ [2 / (U_i + U_j)]^2 + r_{ij}^2 \}^{-1/2}$$

- Mataga-Nishimoto parametrization:

$$V(r_{ij}) = \{ [2 / (U_i + U_j)] + r_{ij} \}^{-1}$$

Model Hamiltonian

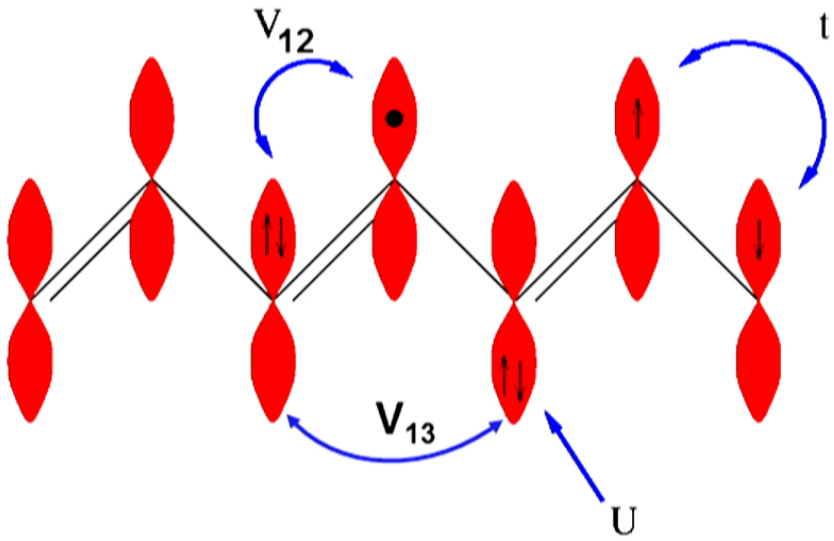

PPP Hamiltonian (1953)

$$\hat{H}_{PPP} = \sum_{<ij>\sigma} t_{ij} \left(\hat{a}^{\dagger}_{i\sigma} \hat{a}_{j\sigma} + H.c.\right) + \sum_{i} (U_i/2) \hat{n}_i (\hat{n}_i - 1)$$

$$+ \sum_{i>j} V(r_{ij}) \left(\hat{n}_i - 1\right) \left(\hat{n}_j - 1\right)$$

Hubbard Model (1964)

- Hückel model + on-site repulsions

$[ii|jj] = 0$ for $i \neq j$;

$[ii|jj] = U_i$ for $i=j$

$$\hat{H}_{Hub} = \hat{H}_o + \sum_i U_i \hat{n}_i (\hat{n}_i - 1)/2$$

Exact Diagonalization (ED) Methods

- Hilbert space of PPP Hamiltonian is finite for molecules.
- PPP model conserves total S and M_S.
- Hilbert space factorized into definite total S and M_S spaces using Rumer-Pauling VB basis.
- Rumer-Pauling VB basis is nonorthogonal, but complete, and linearly independent.
- Recent development allows exploiting full spatial symmetry of any point group.

Z.G. Soos and S. R, (1990) in Valence Bond Theory and Chemical Structure, eds. D.J. Klein and N. Trinajstic, Elsevier, Amsterdam,p.81.
S. Sahoo, SR and D. Sen, Phys. Rev. B 78, 054408 (2008)
S. Sahoo and SR, Int. J. Quantum Chem DOI 10.1002/qua.23097

Exact Diagonalization (ED) Methods

- Hilbert space of PPP Hamiltonian is finite for molecules.
- PPP model conserves total S and M_S.
- Hilbert space factorized into definite total S and M_S spaces using Rumer-Pauling VB basis.
- Rumer-Pauling VB basis is nonorthogonal, but complete, and linearly independent.
- Recent development allows exploiting full spatial symmetry of any point group.

Z.G. Soos and S. R, (1990) in Valence Bond Theory and Chemical Structure, eds. D.J. Klein and N. Trinajstic, Elsevier, Amsterdam,p.81.
S. Sahoo, SR and D. Sen, Phys. Rev. B 78, 054408 (2008)
S. Sahoo and SR, Int. J. Quantum Chem DOI 10.1002/qua.23097

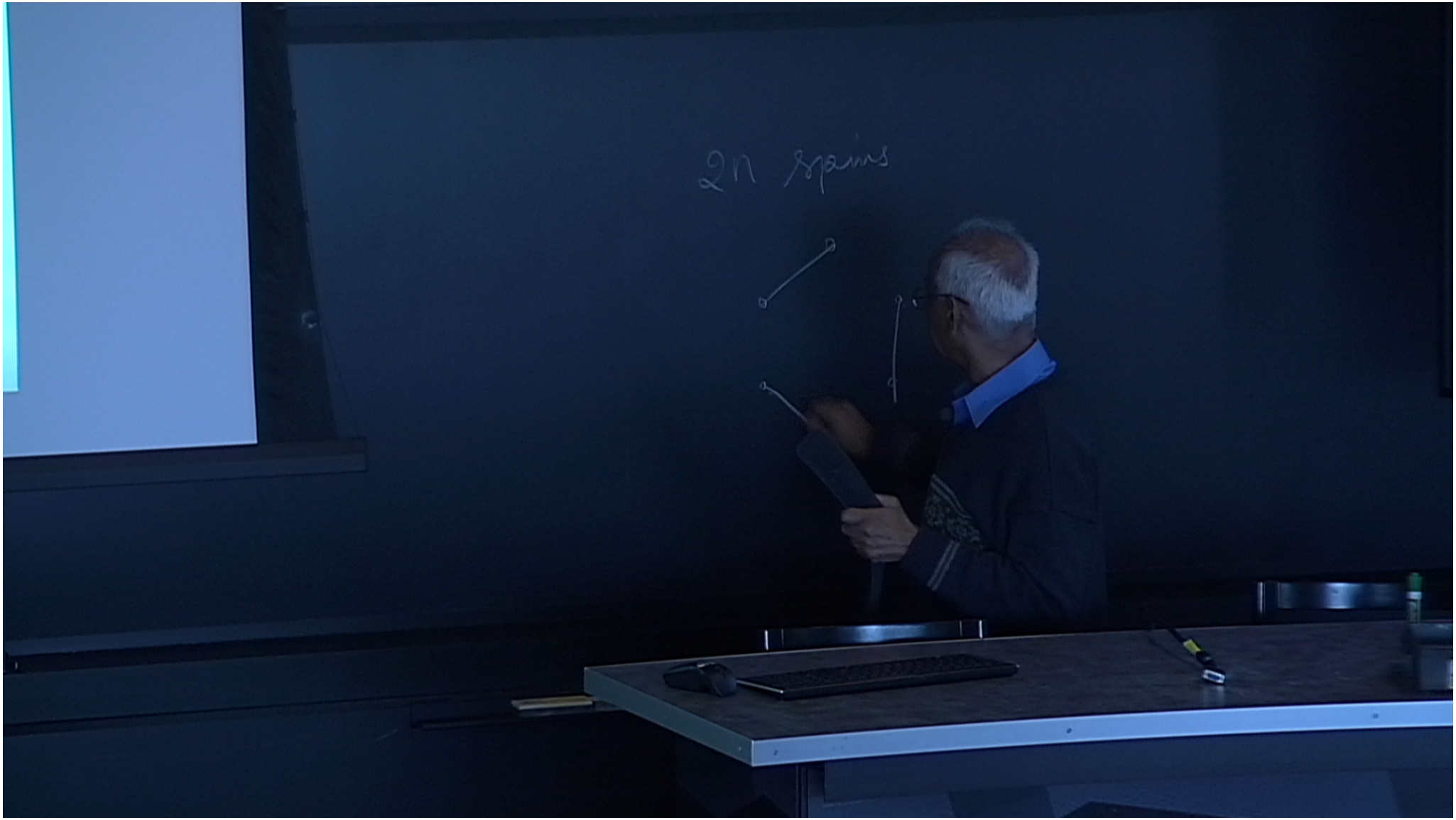
2n Spins

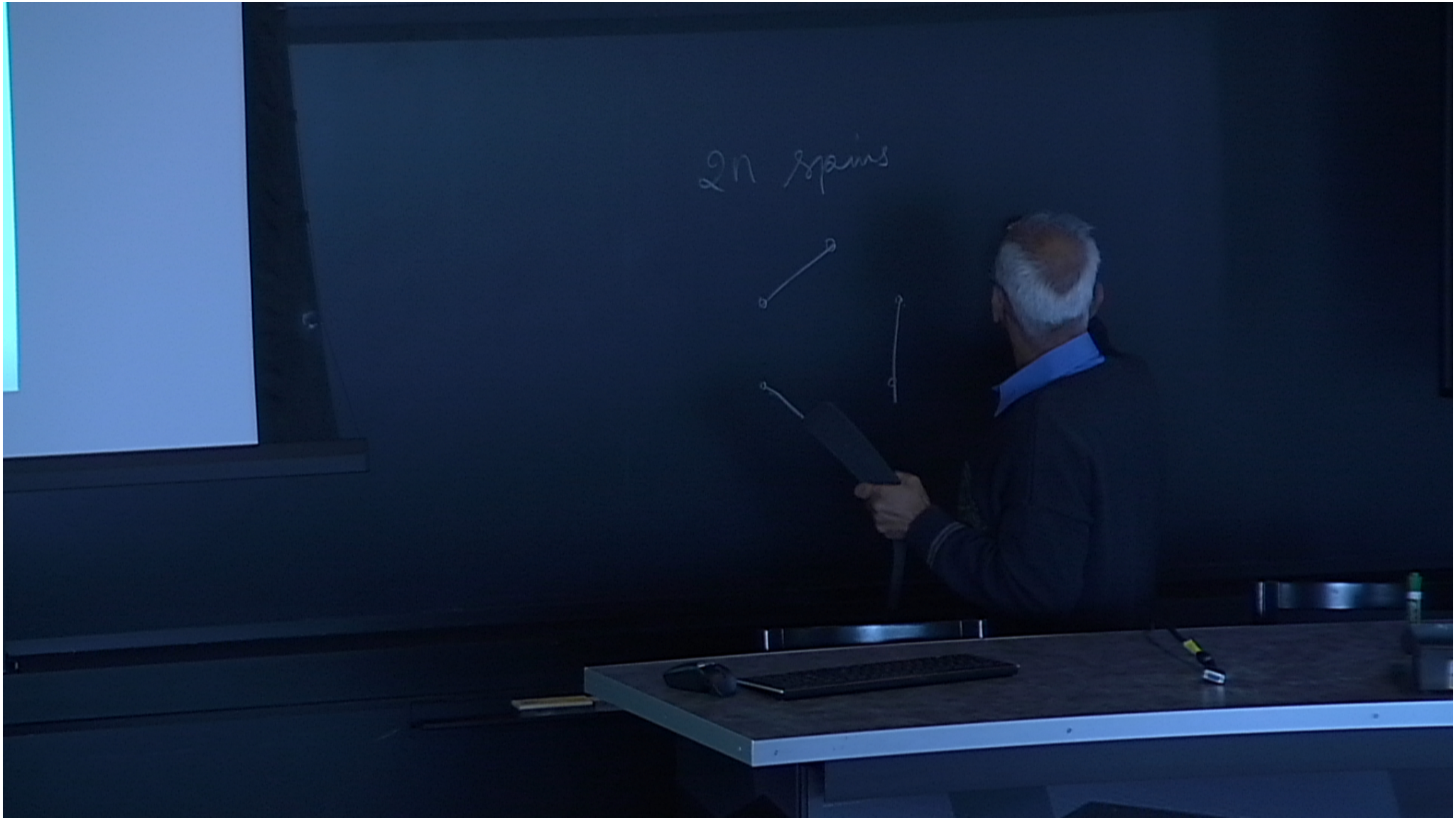
2n spins

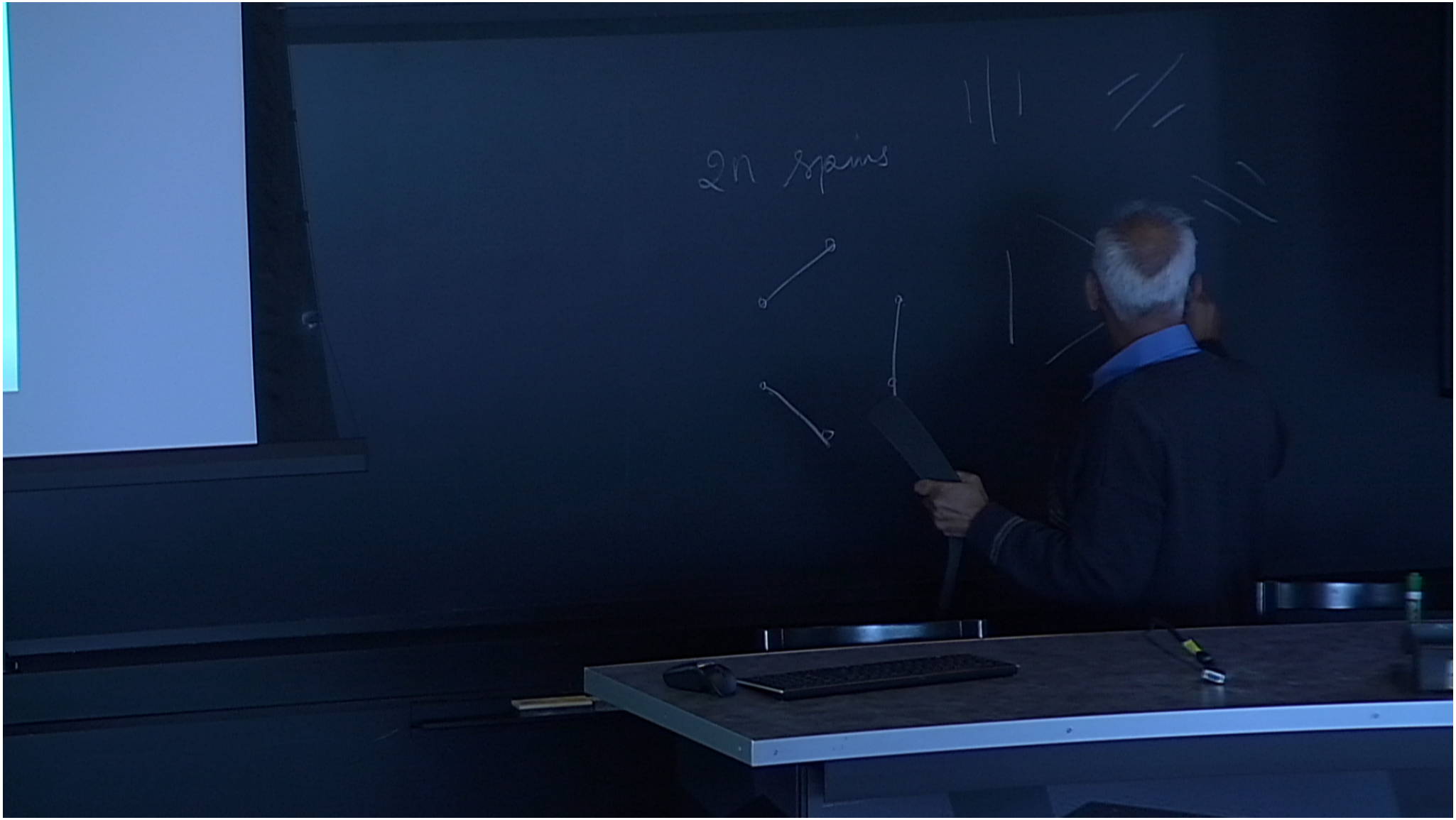
2n spins

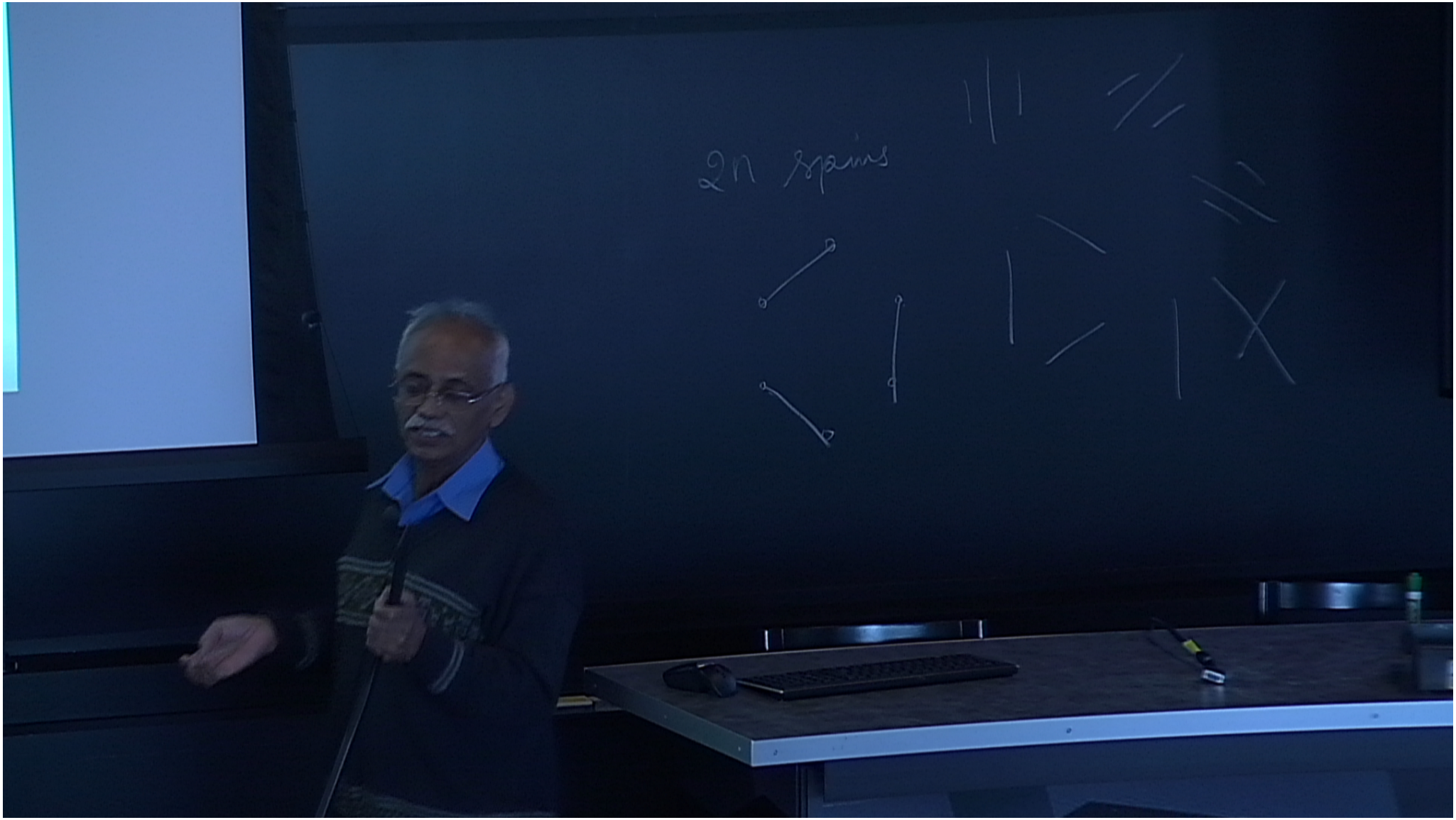
2n spins

Necessity and Drawbacks of ED Methods

- ED methods are size consistent. Good for energy gap extrapolations to thermodynamic or polymer limit.

- Hilbert space dimension explodes with increase in no. of orbitals

  $N_{electrons} = 14, N_{sites} = 14,$ # of singlets = 2,760,615

  $N_{electrons} = 16, N_{sites} = 16,$ # of singlets = 34,763,300

  hence for polymers with large monomers (eg. PPV), ED methods limited to small oligomers.

- ED methods rely on extrapolations. In systems with large π coherence length, ED methods may not be reliable.

- ED methods provide excellent check on approximate methods.

Approximate Methods

- Restricted CI methods
- Coupled Cluster methods
- Quantum Monte Carlo methods
- Renormalization Group Methods
  - Energy eigenvalue based methods
  - Density matrix eigenvalue based methods.

Density matrix based methods.

- Natural orbital basis: eigenfunctions of one particle density matrix with large densities (density matrix eigenvalues) were used as orbitals for CI calculations.
- DMRG uses eigenstates of many-body density matrices to span the Fock space of the many-particle subsystem. Besides it also uses a renormalization procedure to extend the system size.

The Density Matrix Renormalization Group (DMRG) Technique

- DMRG method involves iteratively building a large system starting from a small system.
- The eigenstate of superblock consisting of system and surroundings is used to build density matrix of system.
- Dominant eigenstates ($10^2 \sim 10^3$) of the density matrix are used to span the Fock space of the system.
- The superblock size is increased by adding new sites.
- Very accurate for one and quasi-one dimensional systems such as Hubbard, Heisenberg spin chains and polymers

S.R. White (1992)

Entanglement Entropy and the Area Law.

$$\rho_L |\mu_\alpha\rangle = \mu_\alpha |\mu_\alpha\rangle$$

$$S = -\sum_\alpha \mu_\alpha \log_2 \mu_\alpha$$

Area Law $S \sim$ Area between system and environment.

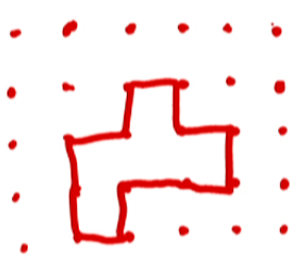

DMRG cut-off $m \sim e^{aS}$

Hence DMRG most accurate for 1-D systems. At criticality, there are log corrections to S leading to higher cut-off for desired accuracy

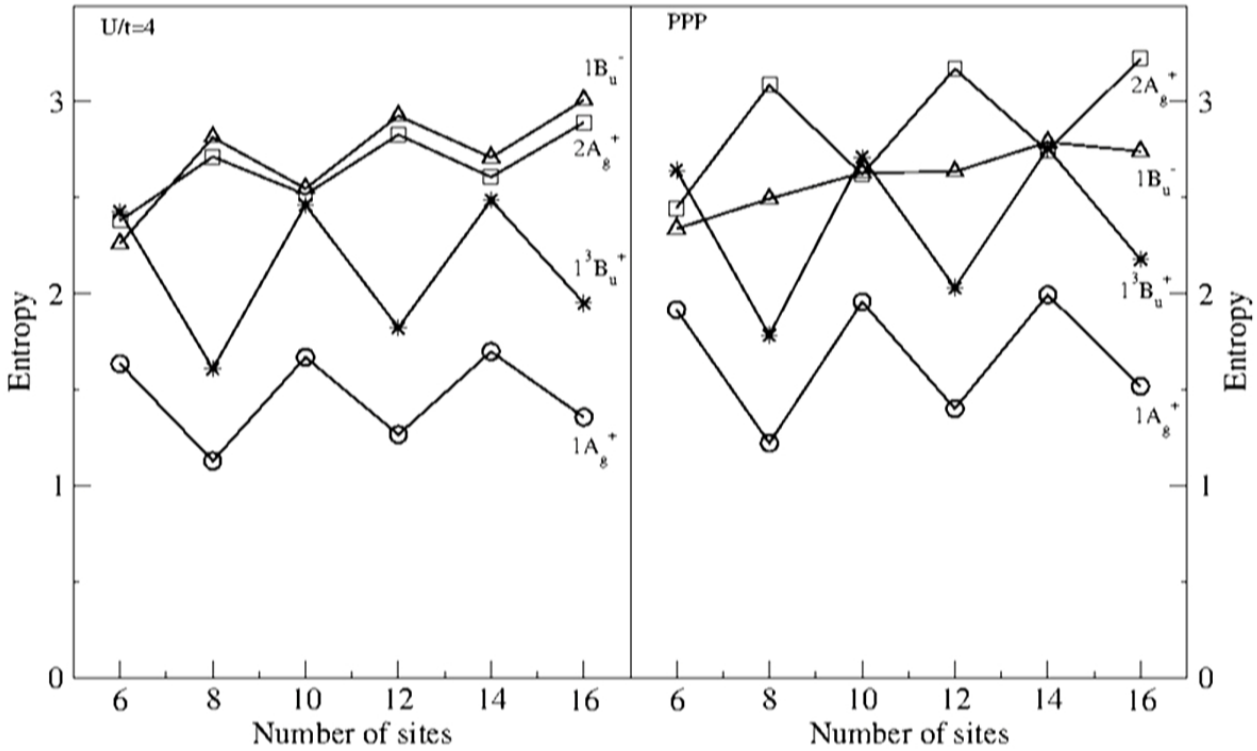

Exact entanglement entropy of Hubbard (U/t=4) and PPP eigenstates of a chain of 16 sites

DMRG technique is accurate for long-range interacting models with diagonal density-density interactions

S. Sahoo, SR and D. Sen, J .Phys. Cond Mat (2012)

DMRG and Matrix Product States

DMRG wavefunction at the end of right sweep

$$\Psi = \sum_{z^{(N-1)}\sigma_N} A^{(N-1)}_{z^{(N-1)},\sigma_N} \left| z^{(N-1)}, \sigma_N \right\rangle$$

$$\left| z^{(N-1)} \right\rangle = \sum_{z^{(N-2)},\sigma_{N-1}} A^{(N-2)}_{z^{(N-1)};\, z^{(N-2)}\sigma_{N-1}} \left| z^{(N-2)}\sigma_{N-1} \right\rangle$$

$$\Psi = \sum_{z^{(N-2)}} \sum_{z^{(N-1)}} \sum_{\sigma_{N-1}} \sum_{\sigma_N} A^{(N-1)}_{z^{(N-1)}\sigma_N} A^{(N-2)}_{z^{(N-1)};\, z^{(N-2)}\sigma_{N-1}} \left| z^{(N-2)}\sigma_{N-1}\sigma_N \right\rangle$$

Continuing

$$\Psi = \sum_{\sigma_1, \sigma_2, \cdots \sigma_N} \sum_{\alpha(1), \alpha(2), \cdots \alpha(N-1)} A^{(1)}_{\alpha(1), \sigma_1} A^{(2)}_{\alpha(2), \alpha(1)\sigma_2} \cdots A^{(N-1)}_{\alpha(N-1), \sigma_N} |\sigma_1 \sigma_2 \cdots \sigma_N\rangle$$

$=$

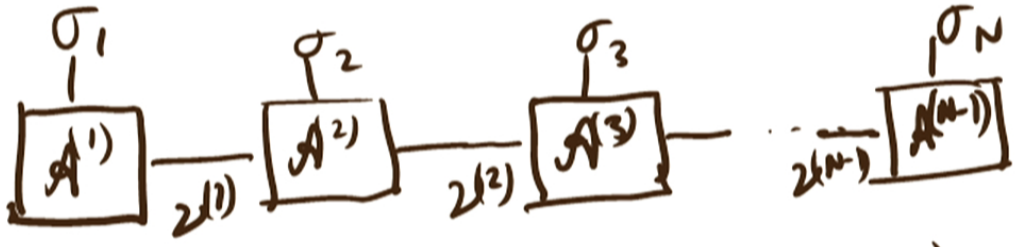

Matrix Product States (MPS)

Symmetrized DMRG Method

Why do we need to exploit symmetries?

- **Important states in conjugated polymers:**

  Ground state ($1^1A^+_g$);
  Lowest dipole excited state ($1^1B^-_u$);
  Lowest triplet state ($1^3B^+_u$);
  Lowest two-photon state ($2^1A^+_g$);
  mA^+_g state (large transition dipole to $1^1B^-_u$);
  nB^-_u state (large transition dipole to mA^+_g)

- **In unsymmetrized methods, too many intruder states between desired eigenstates.**

- **In large correlated systems, only a few low-lying states can be targeted; important states may be missed altogether.**

Symmetries in the PPP and Hubbard Models

Electron-hole symmetry:

- When all sites are equivalent, for a bipartite system, electron-hole or charge conjugation or alternancy symmetry exists, at half-filling.
- At half-filling the Hamiltonian is invariant under the transformation

$$\hat{a}_i^\dagger = \hat{b}_i \text{ ; 'i' on sublattice A}$$

$$\hat{a}_i^\dagger = -\hat{b}_i \text{ ; 'i' on sublattice B}$$

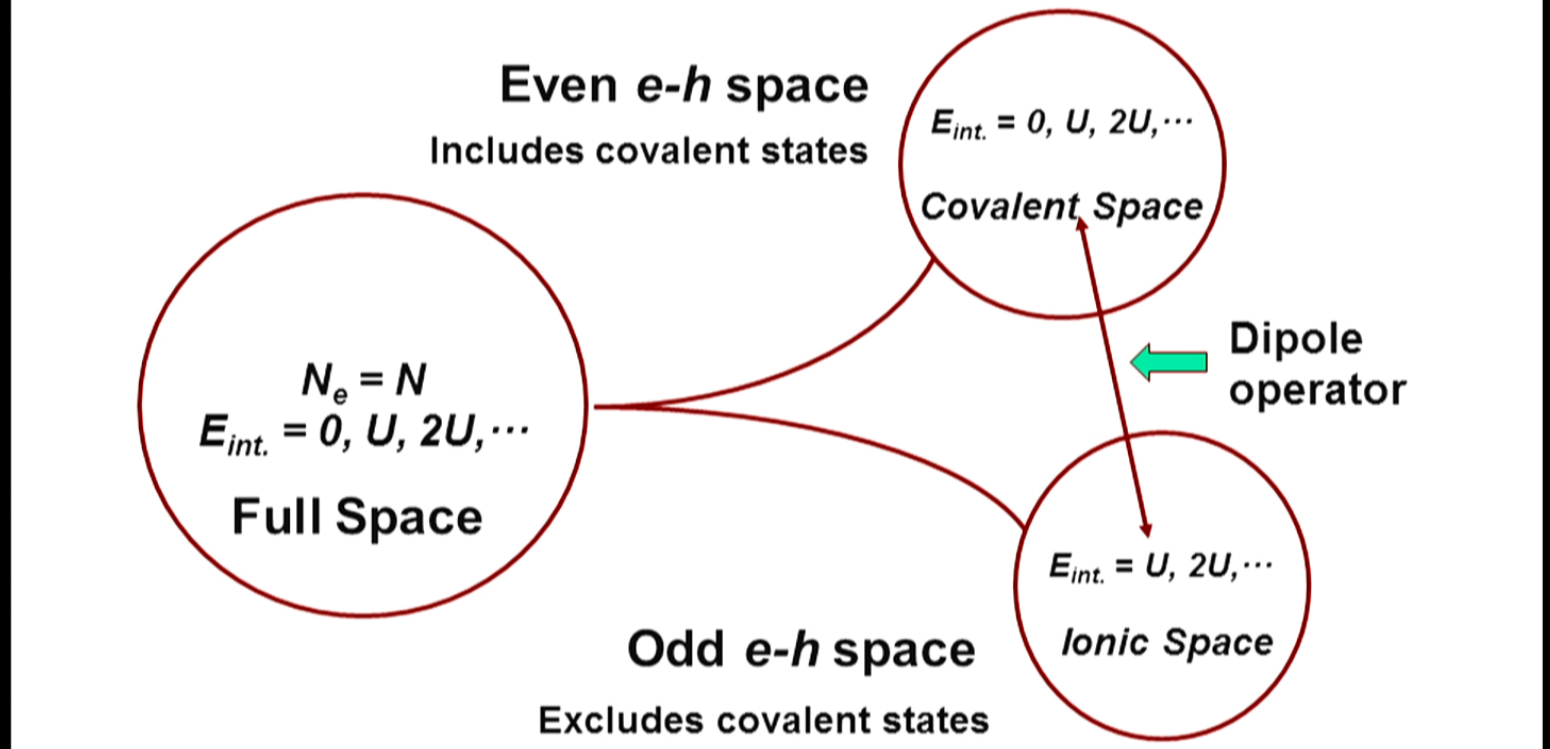

E-h symmetry divides $N = N_e$ space into two subspaces: one containing both 'covalent' and 'ionic' configurations, other containing only ionic configurations.
Dipole operator connects the two spaces.

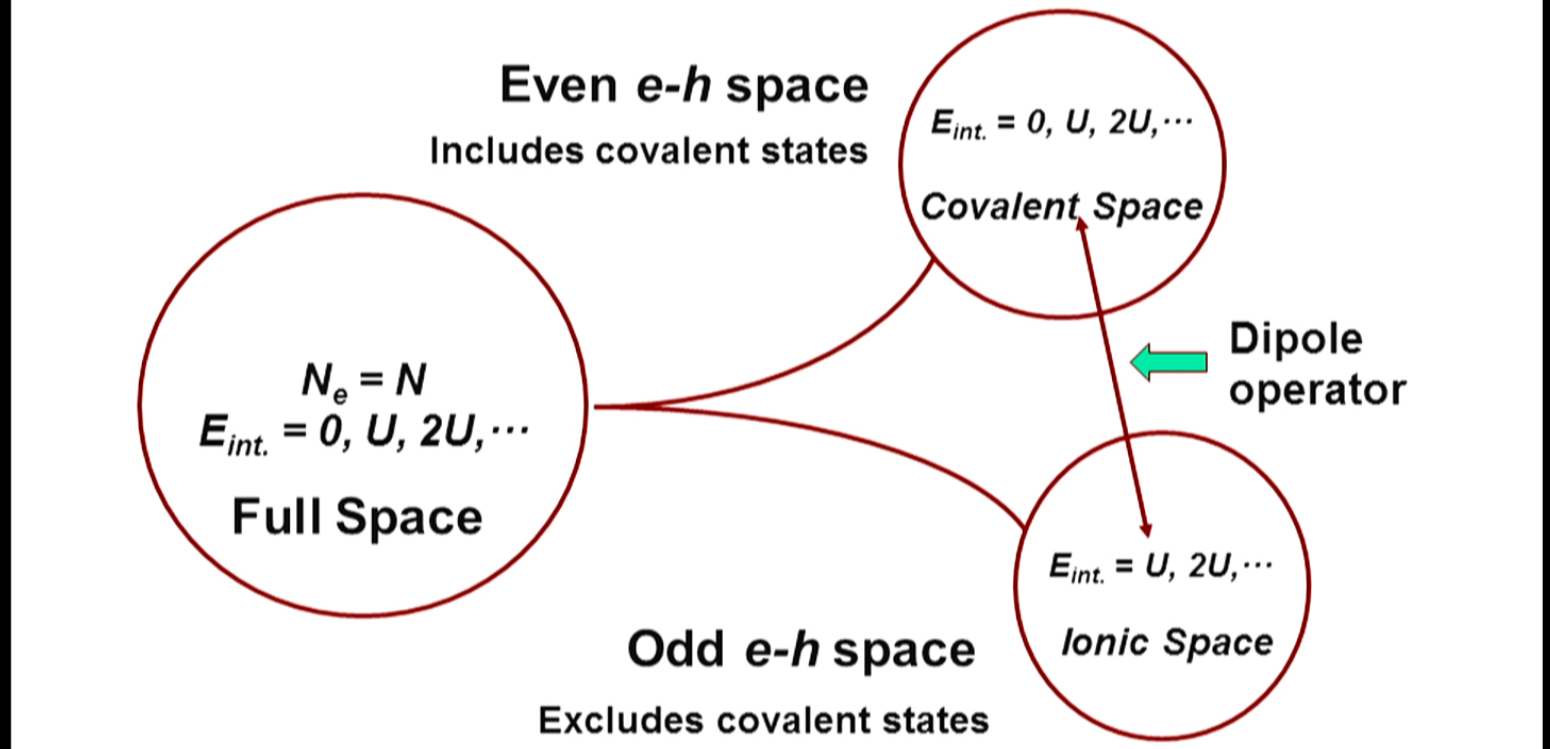

E-h symmetry divides $N = N_e$ space into two subspaces: one containing both 'covalent' and 'ionic' configurations, other containing only ionic configurations.
Dipole operator connects the two spaces.

Spin symmetries

- Hamiltonian conserves total spin and z – component of total spin.

$$[\hat{H},\hat{S}^2] = 0 \; ; \; [\hat{H},\hat{S}_z] = 0$$

- Exploiting invariance of the total $\hat{S}_z$ is trivial, but of the total $\hat{S}^2$ is hard.

- When $M_S^{tot.} = 0$, $\hat{H}$ is invariant when all the spins are rotated about the y-axis by π. This operation flips all the spins of a state and is called spin inversion.

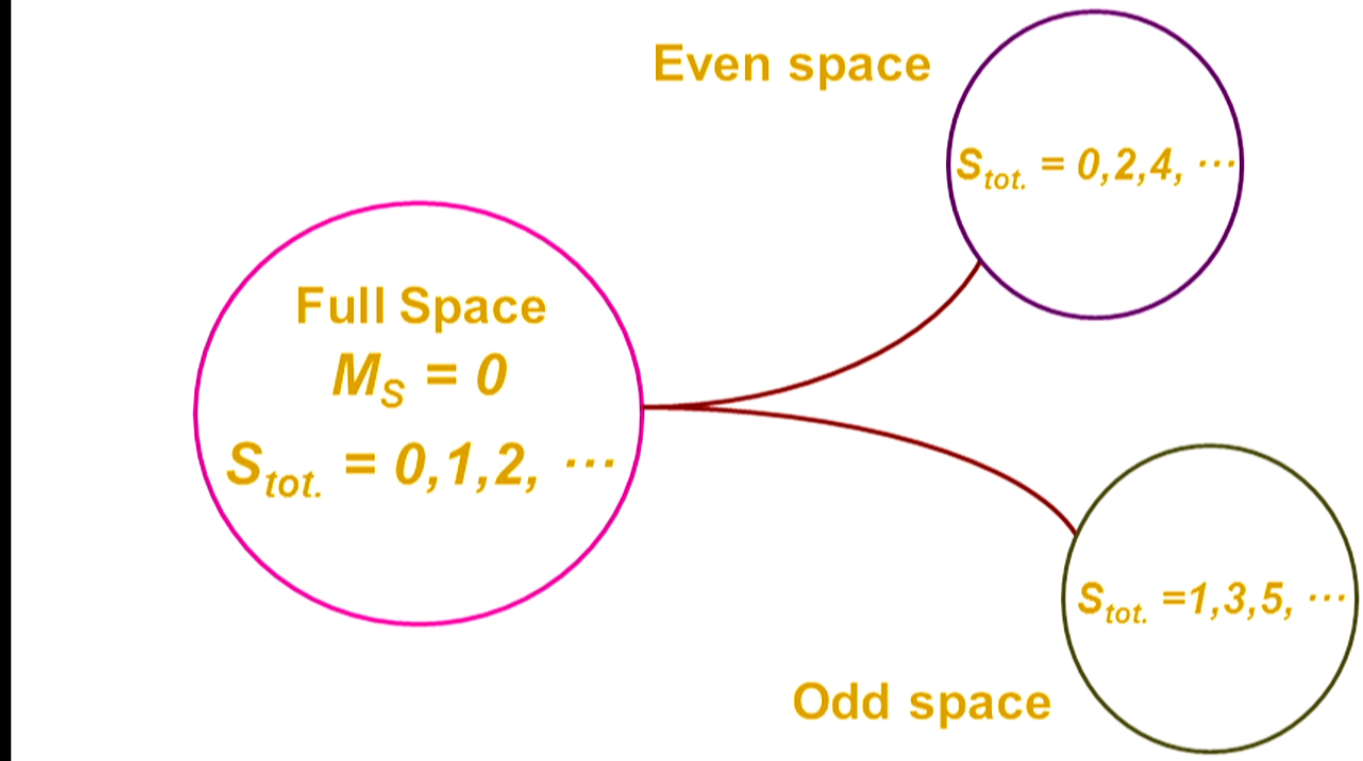

Spin inversion divides the total spin space into spaces of even total spin and odd total spin.

$\hat{C}_2$ Operation on the DMRG basis yields,

$$\hat{C}_2 |\, \mu,\sigma,\sigma',\mu' \rangle = (-1)^{\gamma} \,|\, \mu',\sigma',\sigma,\mu \rangle;$$

$$\gamma = (n_{\sigma'} + n_{\mu'})(n_{\sigma} + n_{\mu})$$

and from this, we can construct the matrix for $\hat{C}_2$.

$\hat{J}$, $\hat{P}$ and $\hat{C}_2$ form an Abelian group

Irr. representations, ${}^{e}A^{+}$, ${}^{e}A^{-}$, ${}^{o}A^{+}$, ${}^{o}A^{-}$, ${}^{e}B^{+}$, ${}^{e}B^{-}$, ${}^{o}B^{+}$, ${}^{o}B^{-}$;

'e' and 'o' imply even and odd under parity;

'+' and '-' imply even and odd under e-h symmetry.

Ground state lies in ${}^{e}A^{+}$,

dipole allowed optical excitation in ${}^{e}B^{-}$,

the lowest triplet in ${}^{o}B^{+}$.

Checks on SDMRG

- Optical gap (E_g) in Hubbard model known analytically. In the limit of infinite chain length, for

$U/t = 4.0$, $E_g^{exact} = 1.2867\ t$; $U/t = 6.0$ $E_g^{exact} = 2.8926\ t$

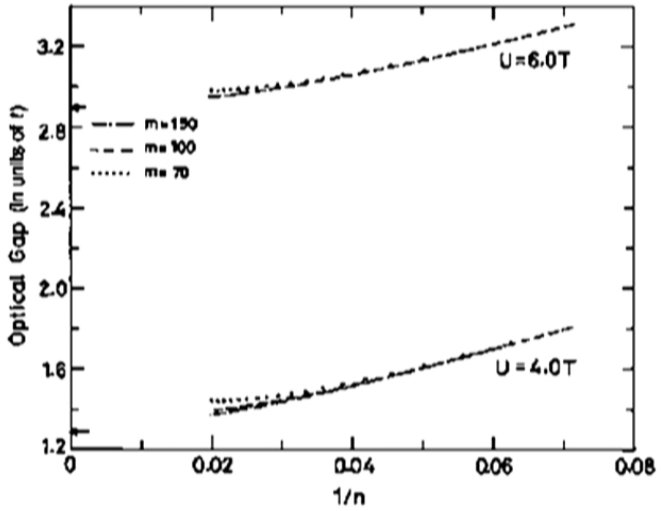

FIG. 1. Optical gap as a function of inverse chain length for Hubbard chains with $U=4.0t$ and $U=6.0t$. m corresponds to the number of density matrix eigenvectors retained in the DMRG procedure. Arrows indicate the model exact gaps for infinite chains.

$E_{g,N\to\infty}^{DMRG} = 1.278$, $U/t = 4$

$E_{g,N\to\infty}^{DMRG} = 2.895$, $U/t = 6$

PRB, 54, 7598 (1996).

The spin gap in the limit U/t $\rightarrow\infty$ should vanish for the Hubbard model.

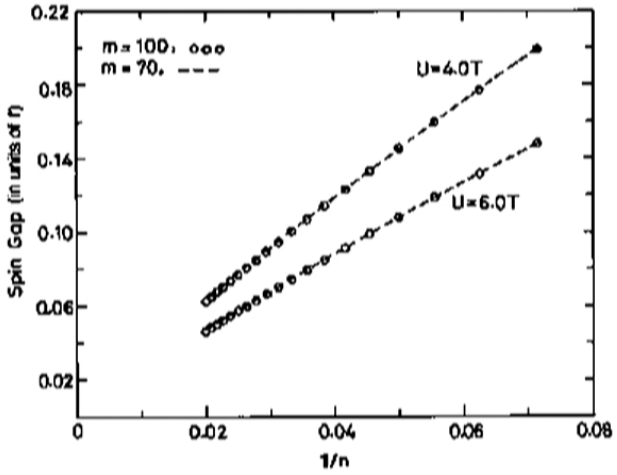

FIG. 2. Spin gap (defined in the text) as a function of $1/m$ for Hubbard chains with $U=4.0t$ and $U=6.0t$. m corresponds to the DMRG cutoff. Model exact spin gaps vanish for infinite chains.

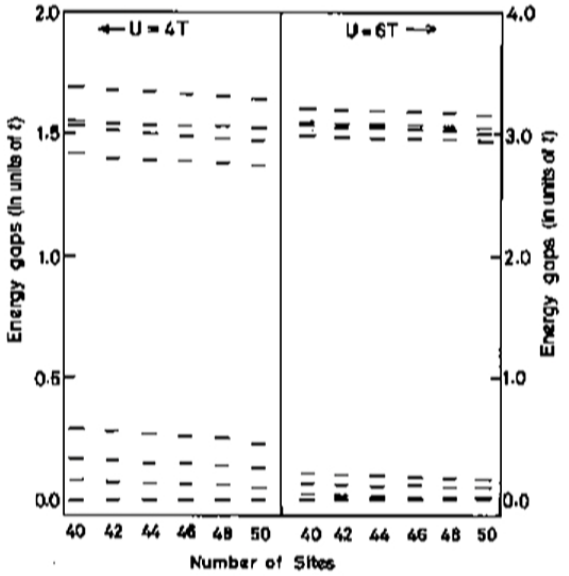

FIG. 3. Energy gaps (measured from the ground state) of the lowest state in each subspace for chain length varying from 40 to 50, for two different values of U/t. The level ordering is $E_{\sigma_A+} < E_{\sigma_A+} < E_{\sigma_B+} < E_{\sigma_B+} < E_{\sigma_B-} < E_{\sigma_A-} < E_{\sigma_B-} < E_{\sigma_A-}$.

PRB, 54, 7598 (1996).

Ordering of Low-lying Excitations

- Two important low-lying excitations in conjugated Polymers:

  lowest one-photon state (1^1B_u)
  lowest two-photon state (2^1A_g).

- Kasha rule in organic photochemistry – fluorescent light emission occurs from lowest excited state.

- Implications for level ordering

  $E(1^1B_u) < E(2^1A_g)$ .... Polymer is fluorescent

  $E(2^1A_g) < E(1^1B_u)$ .... Polymer nonfluorescent

- Level ordering controlled by polymer topology, correlation strength and conjugation length

PRL, 71, 1609 (1993). PRB, 56, 9298 (1997)

Ordering of Low-lying Excitations

- Two important low-lying excitations in conjugated Polymers:

  lowest one-photon state (1^1B_u)
  lowest two-photon state (2^1A_g).

- Kasha rule in organic photochemistry – fluorescent light emission occurs from lowest excited state.

- Implications for level ordering

  $E(1^1B_u) < E(2^1A_g)$ .... Polymer is fluorescent

  $E(2^1A_g) < E(1^1B_u)$ .... Polymer nonfluorescent

- Level ordering controlled by polymer topology, correlation strength and conjugation length

PRL, 71, 1609 (1993). PRB, 56, 9298 (1997)

Small *U/t:*

1^1B_u below 2^1A_g

Large U/t:

2^1A_g below 1^1B_u

Reason:

1^1B_u has no covalent Contribution: Its energy increases with *U/t*.

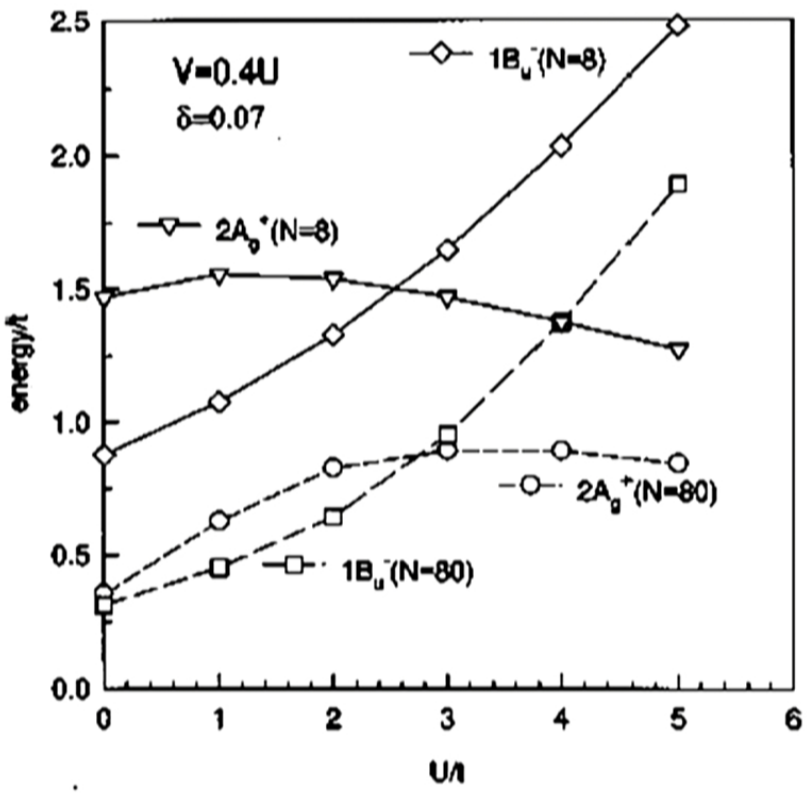

FIG. 1. Crossover on U for δ=0.07.

PRB 56, 9298 (1997)

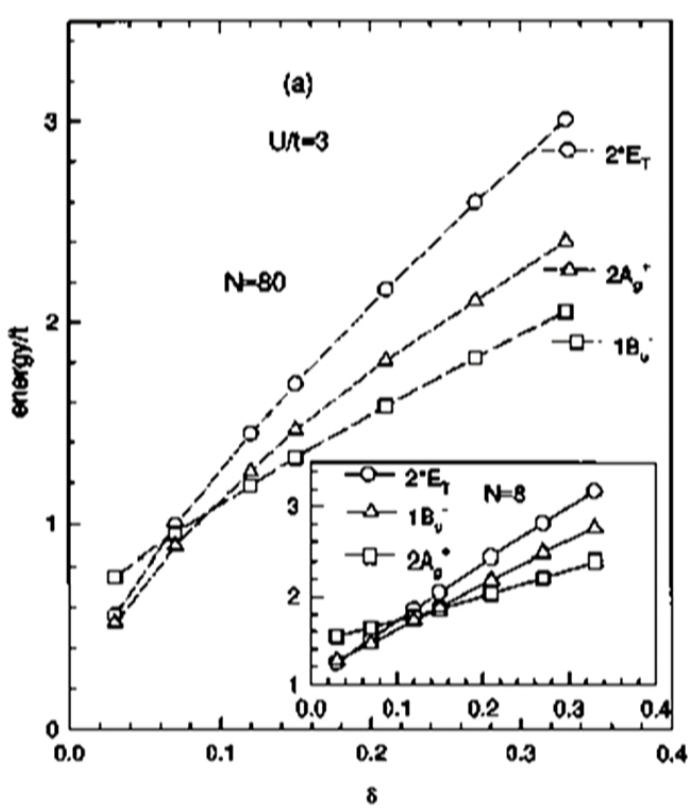

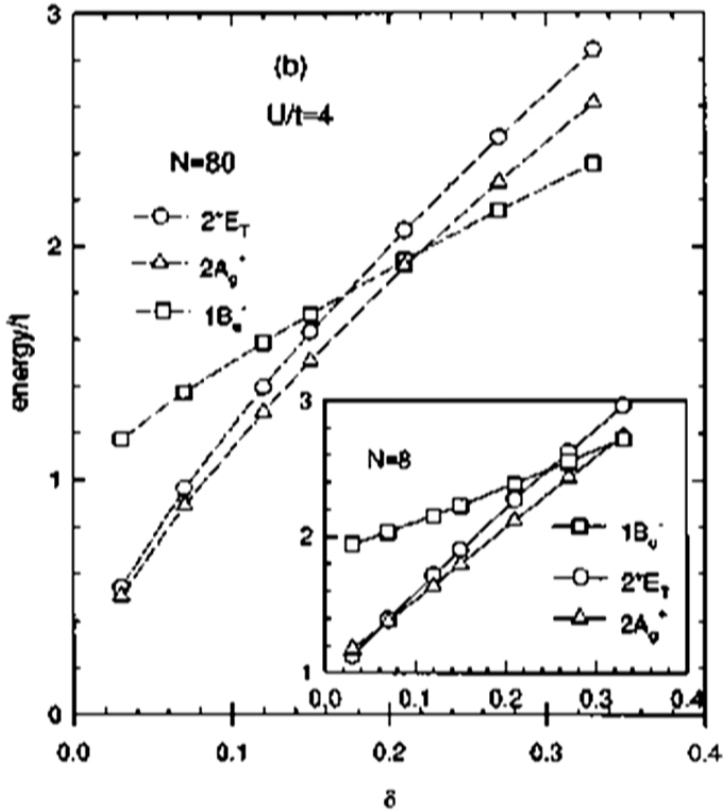

- 1^1B_u - 2^1A_g crossover also occur as a function of δ.
- As U/t increases, crossover occurs at higher value of δ.
- 2^1A_g state described as two triplets at large U/t and small δ

- *2A -1B* crossover occurs as a function of chain length for intermediate *U/t*.

  2A above *1B* for long chains
  2A below *1B* for short chains.

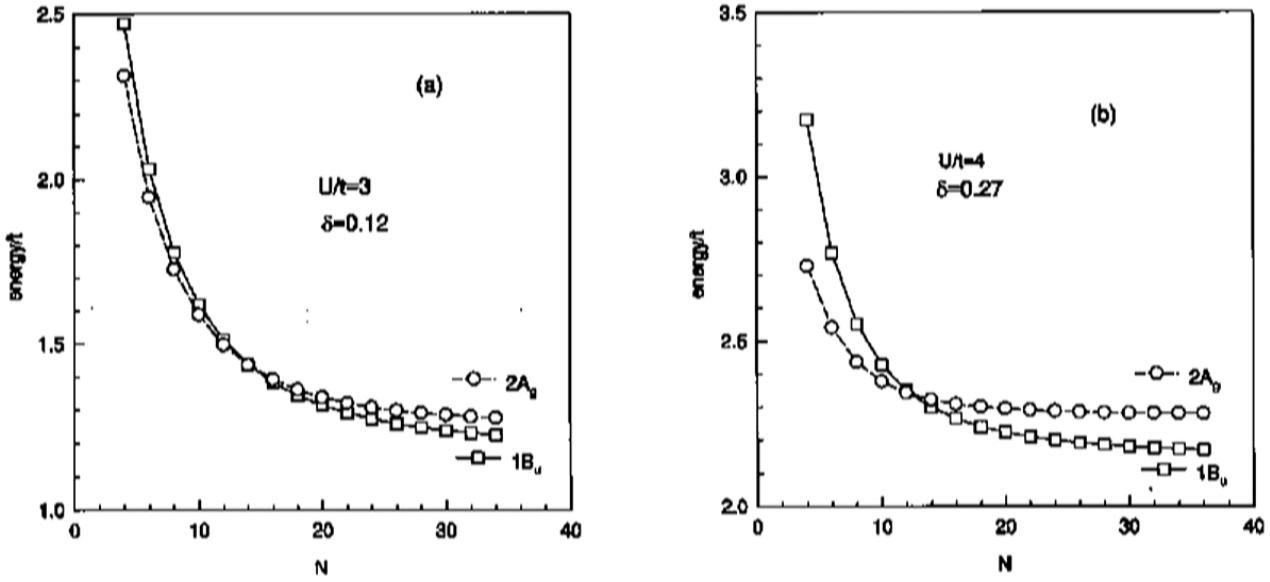

2A state is more localized than *1B* state. As system size increases *1B* descends below *2A*.

PRB 56, 9298 (1997)

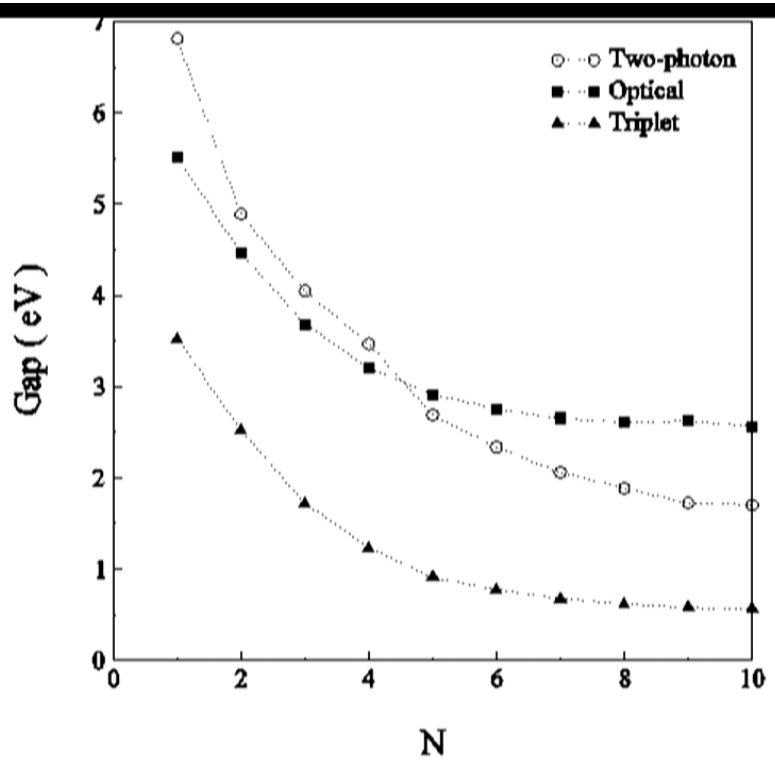

Polyacenes

- Crossover in the two-photon and optical gap at pentacene - experimentally seen.
- One photon state more localized than two photon state.
- Unusually small triplet or spin gap.

Phys. Rev. B 66, 035116 (2002)

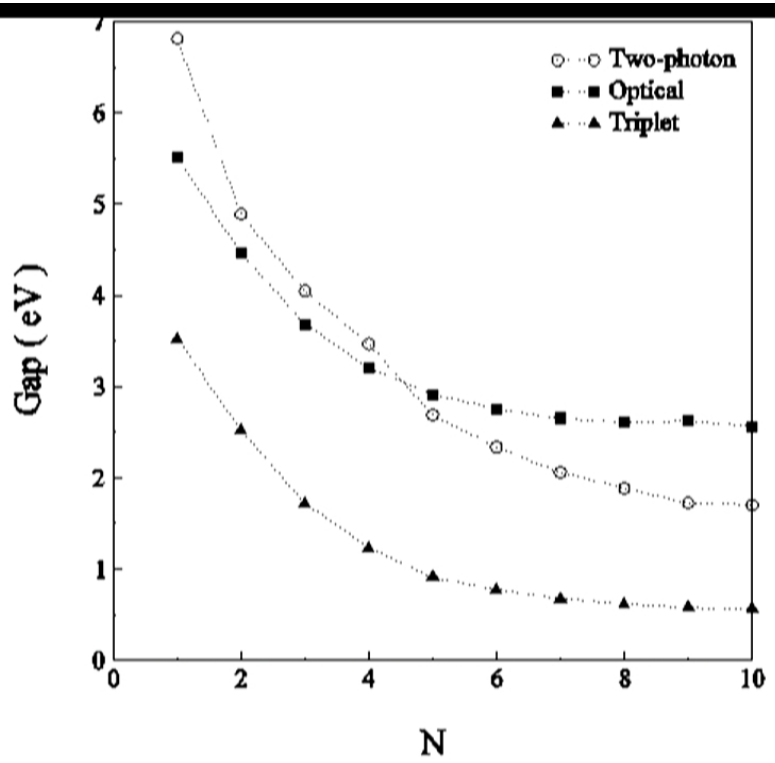

Polyacenes

- Crossover in the two-photon and optical gap at pentacene - experimentally seen.
- One photon state more localized than two photon state.
- Unusually small triplet or spin gap.

Phys. Rev. B 66, 035116 (2002)

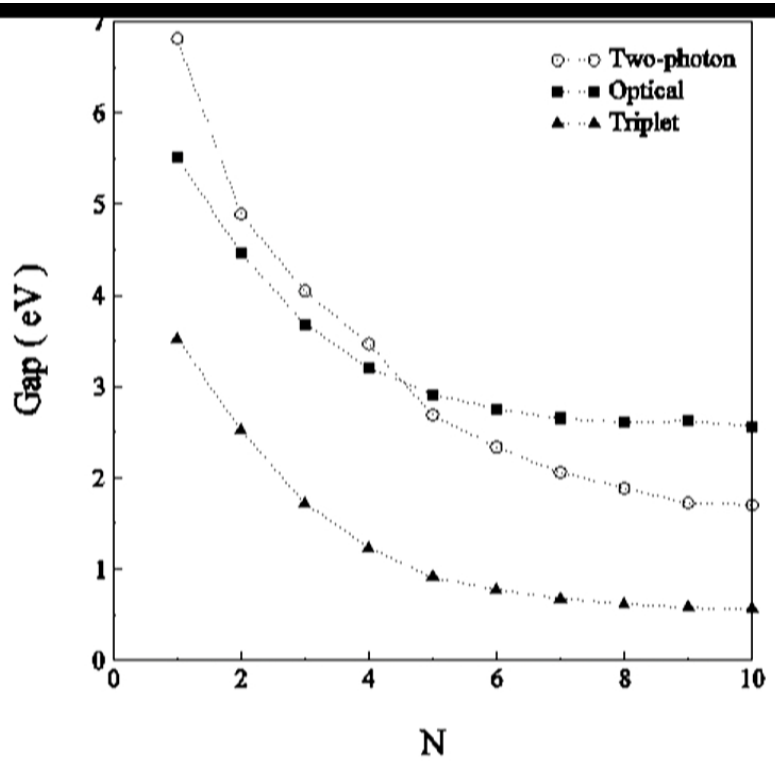

Polyacenes

- Crossover in the two-photon and optical gap at pentacene - experimentally seen.
- One photon state more localized than two photon state.
- Unusually small triplet or spin gap.

Phys. Rev. B 66, 035116 (2002)

Molecular Multiferroics

Fused azulene

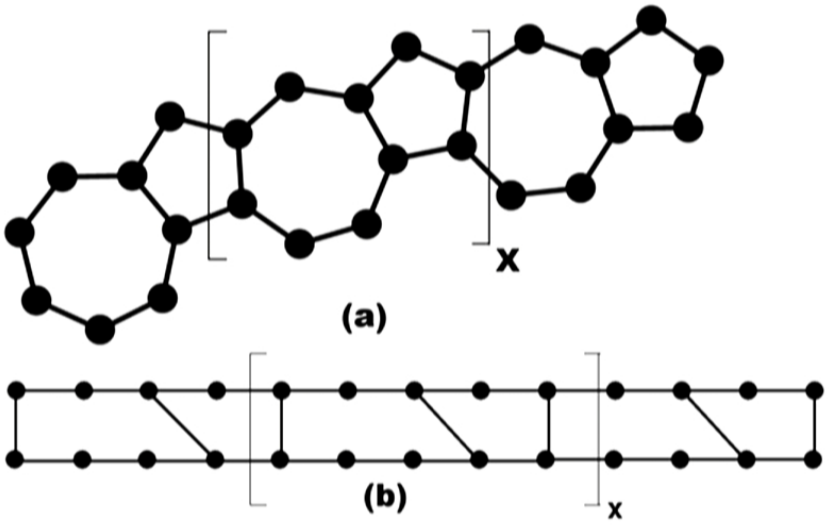

- Azulenes have fused seven and five membered rings.
- Frustration is expected to lower the spin gap
- Hückel (4n+2) rule predicts positive charge on seven membered ring and negative charge on five membered ring

Spin Gaps in Azulene

- $\Delta_1 = E(M_S=1) - E(M_S=0)$
- $\Delta_2 = E(M_S=2) - E(M_S=0)$
- $\Delta_3 = E(M_S=3) - E(M_S=0)$

n is # of azulenes in fused azulene

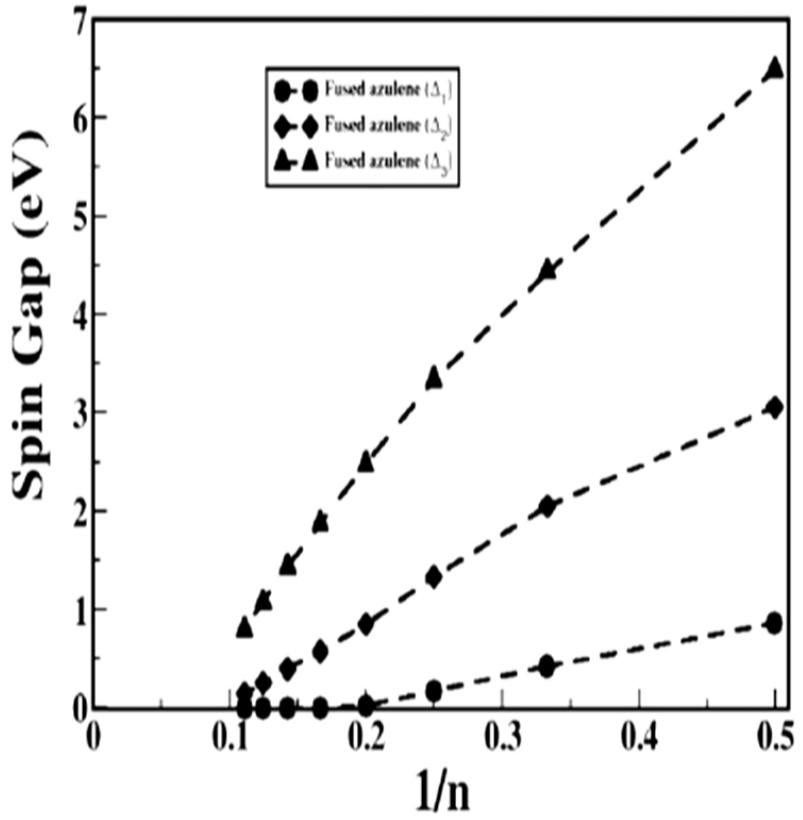

S. Thomas, D. Garcia, K. Hallberg and SR (preprint)

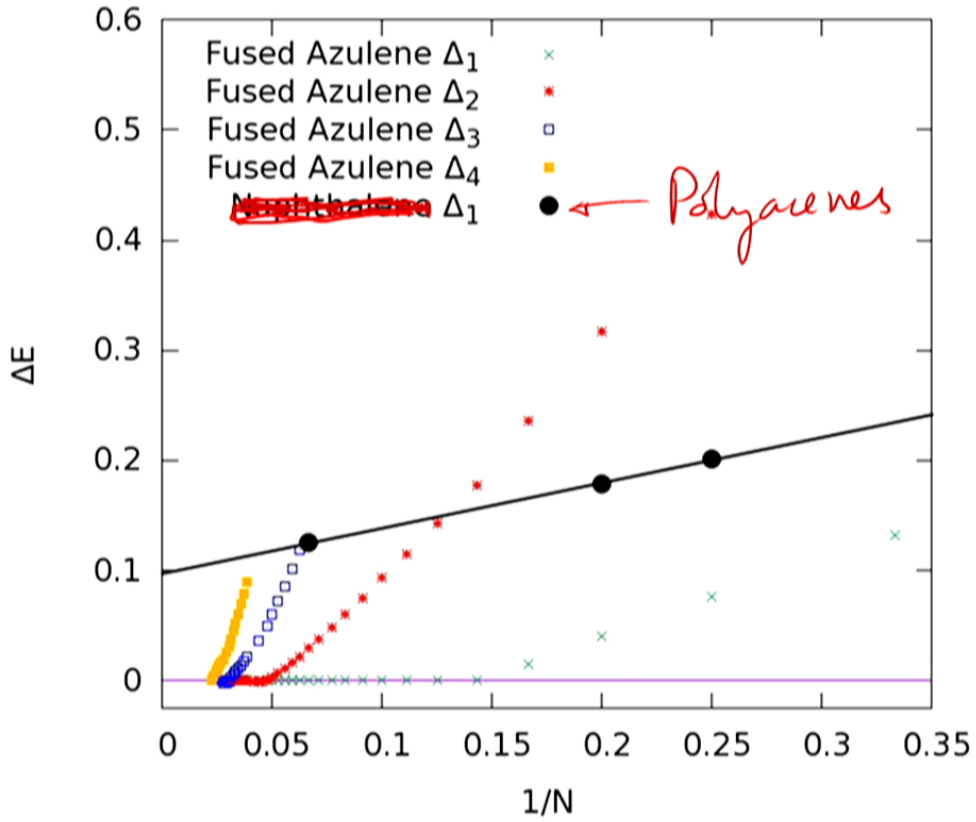

Spin gaps for a s=1/2 Heisenberg antiferromagnetic system on the fused azulene lattice

Spin Gaps in Azulene

- Oligomers up to five azulene units ground state is singlet, S=0.
- Ground state for oligomers with (n>5) is a triplet, S=1.
- Gap Δ_2 appears to vanish for 10 or 11 azulene units, leading to ground state spin S=2.
- From the slopes of the gaps, it appears that in the polymer limit, a ferromagnetic ground state will result.

Spin Gaps in Azulene

- Oligomers up to five azulene units ground state is singlet, S=0.
- Ground state for oligomers with (n>5) is a triplet, S=1.
- Gap Δ_2 appears to vanish for 10 or 11 azulene units, leading to ground state spin S=2.
- From the slopes of the gaps, it appears that in the polymer limit, a ferromagnetic ground state will result.

Charge Distribution in the Oligomers

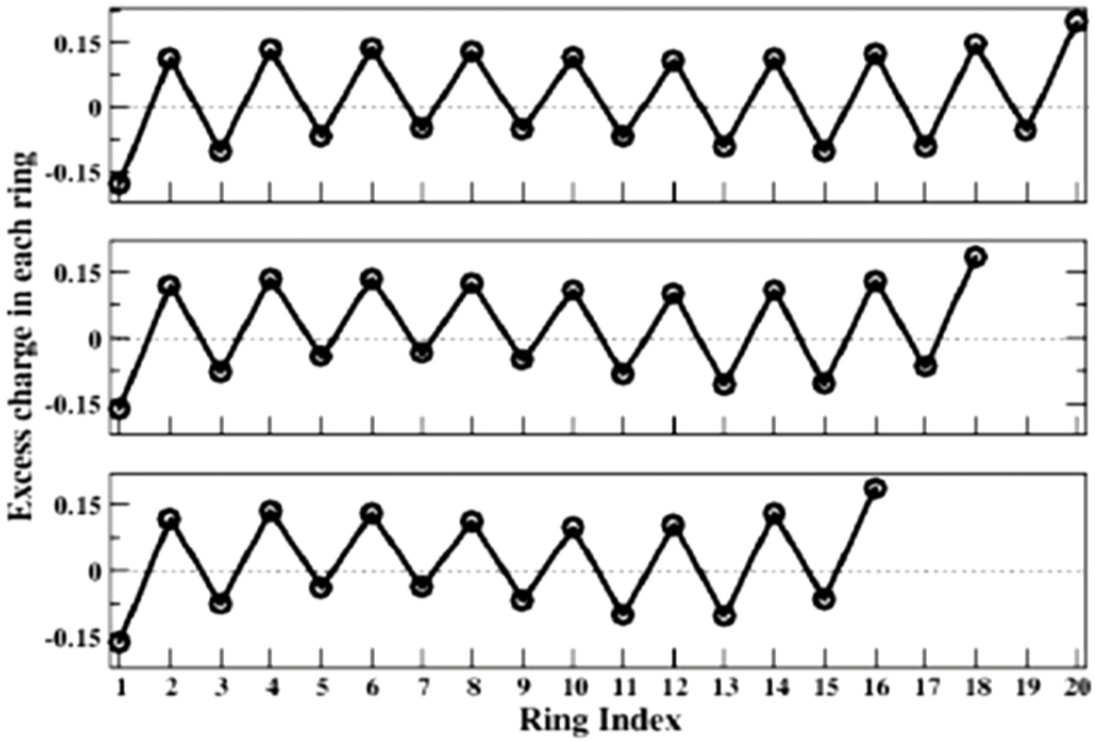

Odd(Even) ring index corresponds to seven(five) membered ring of the azulene.

Computing dynamic response involves calculating

$$I(\omega) = \langle \Psi_0 | \hat{O}^\dagger \frac{1}{E_0 + \omega + i\epsilon - H} \hat{O} | \Psi_0 \rangle$$

where $\hat{O}$ is the operator corresponding to the response property. This can be solved by the Lanczos scheme, the sum over states technique or the correction vector technique

Lanczos method:

We obtain the tridiagonal matrix representation of the Hamiltonian

$$H_L = \begin{pmatrix} c_0 & d_1 & 0 & 0 & 0 & \cdots \\ d_1 & c_1 & d_2 & 0 & 0 & \cdots \\ 0 & d_2 & c_2 & d_3 & 0 & \cdots \\ \vdots & & & & & \\ 0 & 0 & 0 & 0 & \cdots & d_n \; c_n \end{pmatrix}$$

and obtain the ground state of the Hamiltonian $|\tilde{\psi}_0\rangle$. We then repeat the Lanczos scheme with the starting vector

$$|\phi_0\rangle = \hat{O}|\psi_0\rangle / [\langle\psi_0|\hat{O}^\dagger\hat{O}|\psi_0\rangle]^{\frac{1}{2}}$$ to get $\tilde{H}_L$

$$\chi_0 = \langle \phi_0 | \frac{1}{z\mathbb{I} - \tilde{\mathcal{H}}_L} | \phi_0 \rangle$$

$$= \langle \Psi_0 | \hat{O}^\dagger \frac{1}{z\mathbb{I} - \tilde{\mathcal{H}}_L} \hat{O} | \Psi_0 \rangle / [\langle \phi_0 | \phi_0 \rangle]^{1/2}$$

with $\tilde{\mathcal{H}}_L = \begin{pmatrix} a_0 & b_1 & 0 & 0 & \cdots \\ b_1 & a_1 & b_2 & 0 & \cdots \\ 0 & b_2 & a_2 & b_3 & \cdots \\ \vdots & & & & \\ 0 & 0 & \cdots & b_n & a_n \end{pmatrix}$

$$I(\omega) = -\frac{1}{\pi} \mathrm{Im} \left(\frac{\langle \Psi_0 | \hat{O}^\dagger \hat{O} | \Psi_0 \rangle}{z - a_0 - \cfrac{b_1^2}{z - a_1 - \cfrac{b_2^2}{z - a_2 - \cfrac{b_3^2}{\ddots}}}} \right)$$

Karen Hallberg
PRB 1995

Lanczos Technique is numerically fast and efficient, but not very accurate as it involves truncation of the Hilbert space.

In quantum chemistry literature $I(\omega)$ is obtained by computing a small ($10^2 \sim 10^3$) excited states of the Hamiltonian $|R\rangle$ and obtaining $I(\omega)$ as

$$I(\omega) = -\frac{1}{\pi} \mathrm{Im}\left[\frac{\langle \Psi_0 | \hat{O}^\dagger | R\rangle\langle R | \hat{O} | \Psi_0 \rangle}{E_R - E_0 + \hbar\omega + i\epsilon}\right]$$

The Correction Vector Technique

We can define a vector $\varphi^{(1)}(\omega)$ as

$$(\hat{H} - E_0 - \hbar\omega - i\epsilon)\,|\varphi^{(1)}(\omega)\rangle = \hat{O}\,|\psi_0\rangle$$

If $\varphi^{(1)}(\omega)$ is expanded in the eigenstates of $\hat{H}$ as

$$\varphi^{(1)}(\omega) = \sum_R C_R\,|R\rangle$$

with $\hat{H}\,|R\rangle = E_R\,|R\rangle$, we can show that

$$C_R = \frac{\langle R|\hat{O}|\psi_0\rangle}{E_R - E_0 - \hbar\omega - i\epsilon}$$

Lanczos Technique is numerically fast and efficient, but not very accurate as it involves truncation of the Hilbert space. In quantum chemistry literature $I(\omega)$ is obtained by computing a small ($10^2 \sim 10^3$) excited states of the Hamiltonian $|R\rangle$ and obtaining $I(\omega)$ as

$$I(\omega) = -\frac{1}{\pi} \mathrm{Im}\left[\frac{\langle \Psi_0 | \hat{O}^\dagger | R\rangle\langle R | \hat{O} | \Psi_0 \rangle}{E_R - E_0 + \hbar\omega + i\epsilon}\right]$$

The Correction Vector Technique

We can define a vector $\varphi^{(1)}(\omega)$ as

$$(\hat{H} - E_0 - \hbar\omega - i\epsilon)\,|\varphi^{(1)}(\omega)\rangle = \hat{O}\,|\psi_0\rangle$$

If $\varphi^{(1)}(\omega)$ is expanded in the eigenstates of $\hat{H}$ as

$$\varphi^{(1)}(\omega) = \sum_R C_R\,|R\rangle$$

with $\hat{H}\,|R\rangle = E_R\,|R\rangle$, we can show that

$$C_R = \frac{\langle R|\hat{O}|\psi_0\rangle}{E_R - E_0 - \hbar\omega - i\epsilon}$$

and $I(\omega) = \frac{-1}{\pi} \mathrm{Im} \langle \psi_g | \hat{O} | \phi^{(1)}(\omega) \rangle$

Since we already know $\hat{H}$ in a chosen basis (DMRG basis, VB basis, Slater determinants), we can solve for $\phi^{(1)}(\omega)$ in that basis. If

$$\phi^{(1)}(\omega) = \sum_k c_k |k\rangle$$

then we can write the equation for $\phi^{(1)}(\omega)$ as

$$A\vec{c} = \vec{b}$$

$$A_{ij} = (E_0 + \hbar\omega + i\epsilon)\delta_{ij} - H_{ij}$$

and $b_i = \sum_j O_{ij} a_j$; $|\Psi_0\rangle = \sum_j a_j |j\rangle$

Solution $\vec{C}$ can be obtained in the full basis of the Hamiltonian and

$I(\omega) = -\frac{1}{\pi} \mathrm{Im} \langle \Psi_j | \hat{O}^\dagger | \varphi^{(1)}(\omega) \rangle$ in exact within the chosen basis

Solution of $A\vec{C} = \vec{b}$ can be obtained by a small matrix algorithm similar to Davidson's

SR J. Comp. Chem 11, 545 (1990)

If $\hat{O}$ is the dipole displacement operator, $\hat{\mu}$, then polarizability

$$\alpha_{ij}(\omega) = \frac{1}{2}\left[\langle \phi_i^{(1)}(\omega) | \hat{\mu}_j | \psi_g \rangle + \langle \phi_i^{(1)}(-\omega) | \hat{\mu}_j | \psi_g \rangle\right]$$

To obtain higher order nonlinear response coefficients, we define the next order equation

$$(\hat{\mathcal{H}} - E_0 + \hbar\omega_2 + i\epsilon)\, \phi_{ij}^{(2)}(\omega_1, \omega_2) = \hat{\mu}_i\, \phi_j^{(1)}(\omega_1)$$

and $$\gamma_{ijkl} = \hat{P} \langle \phi_i^{(1)}(\omega_3) | \hat{\mu}_j | \phi_{kl}^{(2)}(-\omega_1 - \omega_2, -\omega_1) \rangle$$

where $\hat{P}$ is intrinsic permutation symmetry operator

In the DMRG scheme, we can improve the accuracy by constructing an average density matrix which includes the density matrix from $\varphi^{(1)}(\omega)$.

The method, though more accurate than the Lanczos scheme, is more computationally intensive. Involves solving algebraic equations for every ω.

Synth. Metals (1997); J. Chem. Phys. (1989). Chem. Phys. Letts. (1988).

To test the technique, we compare the rotationally averaged linear polarizability $\bar{\alpha}$ and THG coefficient $\bar{\gamma}$

$$\bar{\alpha} = \frac{1}{3}\sum_{i=1}^{3}\alpha_{ii}; \quad \bar{\gamma} = \frac{1}{15}\sum_{i,j=1}^{3}(2\gamma_{iijj} + \gamma_{ijji})$$

Computed at $\omega = 0.1t$ exactly for a Hubbard chain of 12 sites at $U/t=4$ with DMRG computation with $m=200$

$\bar{\alpha}_{exact}$	$\bar{\alpha}_{DMRG}$	$\bar{\gamma}_{exact}$	$\bar{\gamma}_{DMRG}$
5.343	5.317	598.3	591.1

The dominant α (α_{xx}) is 14.83 (exact) and 14.81 (DMRG) and γ (γ_{xxxx}) 2873 (exact) and 2872 (DMRG).

α in 10^{-24} esu and γ in 10^{-36} esu in all cases

PRB, 59, 14827 (1999).

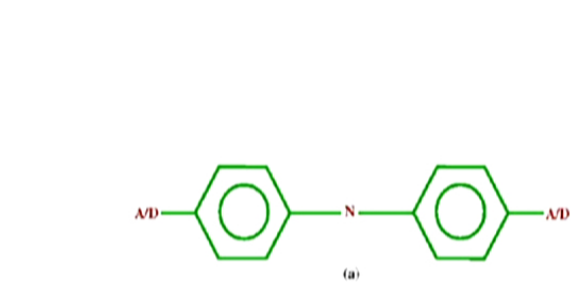

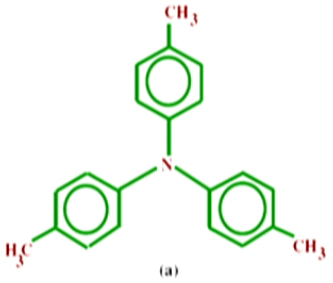

TTA

TSA

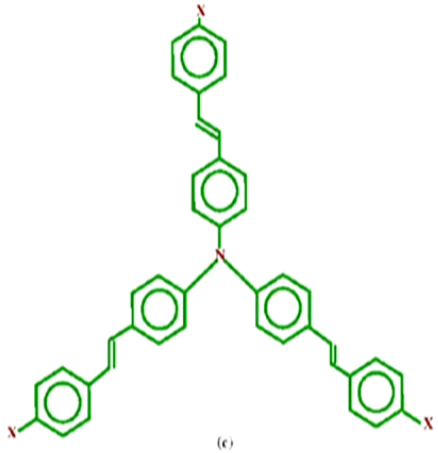

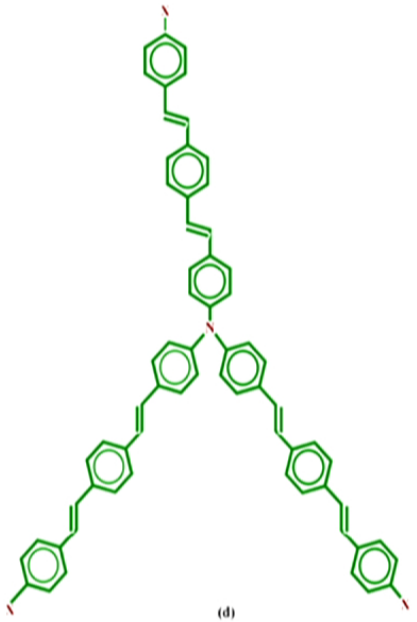

TSA1

Table 6.4: Calculation of tumbling averaged polarizabilities and hyperpolarizabilities by two-state model (TSM) and correction vector (CV) techniques.

Model	System	$\bar{\alpha}$ ($\times 10^{-23}$ esu)	$\bar{\beta}_i$ ($\times 10^{-30}$ esu)			$\lvert\bar{\beta}\rvert$ ($\times 10^{-30}$ esu)
			β_x	β_y	β_z	
TSM	TTA	29.00	17.20	20.42	-19.70	33.18
	TSA	106.81	17.60	190.40	-131.20	231.90
	TSA1	139.05	-65.82	208.09	242.06	325.92
CV	TTA	163.97	13.02	-19.24	15.93	28.17
	TSA	465.13	15.41	22.34	-29.78	40.29
	TSA1	642.39	-28.11	16.35	38.69	50.54

S. Mukhopadhyay and SR J. Chem. Phys. 131, 074111 (2009)

Real Time Dynamics

Important to understand processes such as

spin-charge separation

electron-hole recombination

Fluorescent Resonant Energy Transfer

- - - -

- - - - -

Study involves propagating a wavepacket $\Psi(0)$ at zero time using time dependent Schrödinger Equation

$$i\hbar \frac{\partial \Psi}{\partial t} = \hat{H}\Psi$$

Ψ is the desired wavepacket, eg. a hole doped at site 1 in the ground state

$$|\Psi\rangle = a_{1\uparrow}|\Phi_g\rangle$$

we follow the time evolution of Ψ and

Calculate evolution of properties such as

$$n_i(t) \doteq \langle \Psi(t)|\hat{n}_{i\sigma} + \hat{n}_{i,-\sigma}|\Psi(t)\rangle$$

and

$$s_i^z(t) = \langle \Psi(t)|\hat{n}_{i\sigma} - \hat{n}_{i,-\sigma}|\Psi(t)\rangle$$

at various sites 'i' of the system

Multistep Differencing (MSD)Techniques

MSD4:

$$e^{i2\hat{H}\Delta t/\hbar} - e^{-i2\hat{H}\Delta t/\hbar} = \frac{i\hat{H}\Delta t}{\hbar}(-4+\frac{8}{3}\frac{\hat{H}^2\Delta t^2}{\hbar^2}) + O(\Delta t^5)$$

$$\frac{\hat{H}^2\Delta t^2}{\hbar^2} = 2 - e^{i\hat{H}\Delta t/\hbar} - e^{-i\hat{H}\Delta t/\hbar}$$

$$e^{-i2\hat{H}\Delta t/\hbar} \approx e^{i2\hat{H}\Delta t/\hbar} - \frac{4i\hat{H}\Delta t}{3\hbar}[I + 2(e^{i\hat{H}\Delta t/\hbar} + e^{-i\hat{H}\Delta t/\hbar})]$$

operating on $\psi(0)$

$$\Psi(t+2\Delta t) \approx \Psi(t-2\Delta t) - \frac{4i\hat{H}\Delta t}{3\hbar}[\Psi(t) + 2(\Psi(t-\Delta t) + \Psi(t+\Delta t))]$$

Fast - involves only one sparse matrix multiplication for time propagation. Time dependent quantities evaluated as <O(t)> = <ψ(t)|O|ψ(t)>.

63

The DMRG space at time $t=0$ rapidly fails to satisfactorily describe the wave packet at later times $t > t_0$

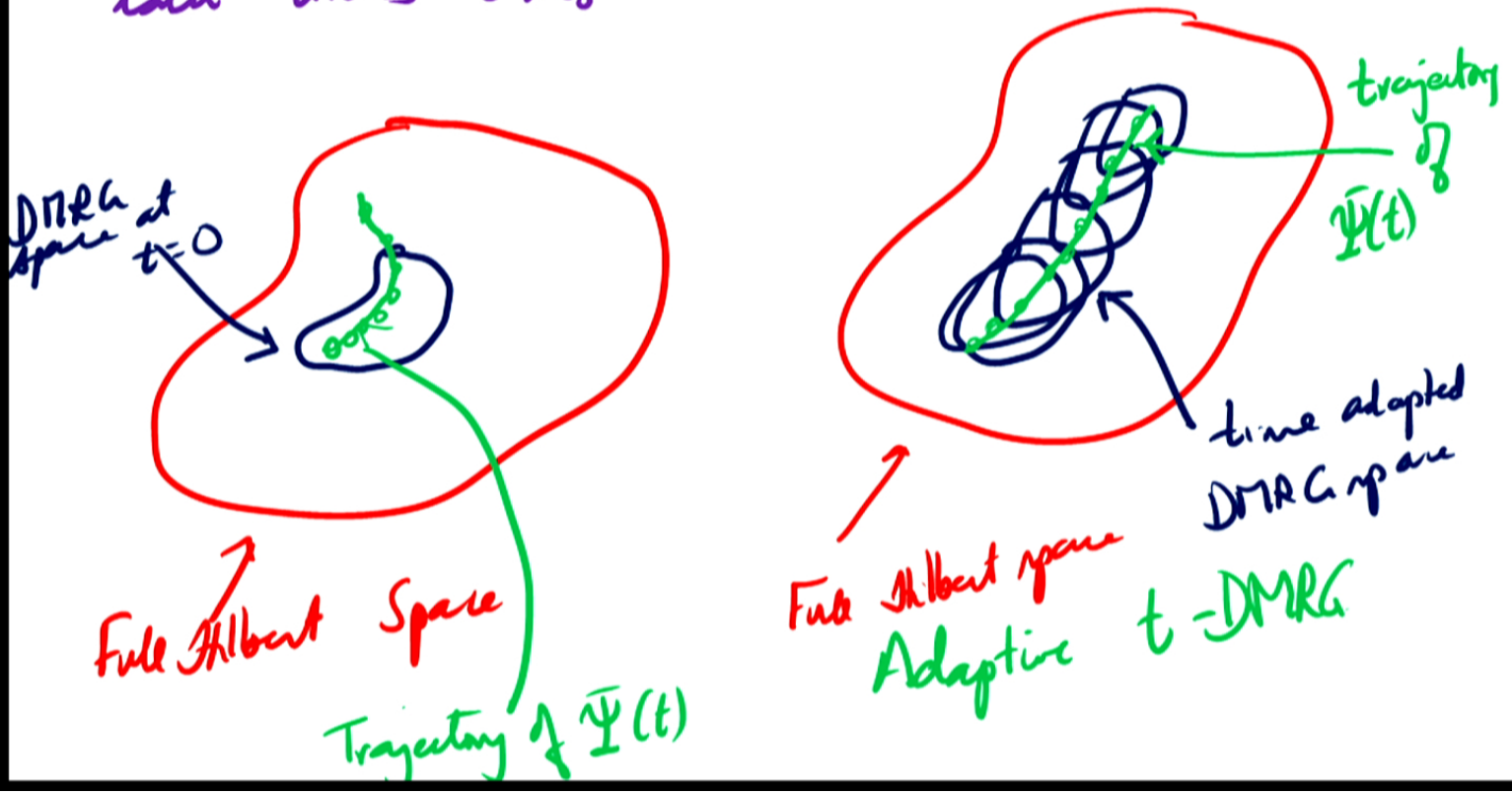

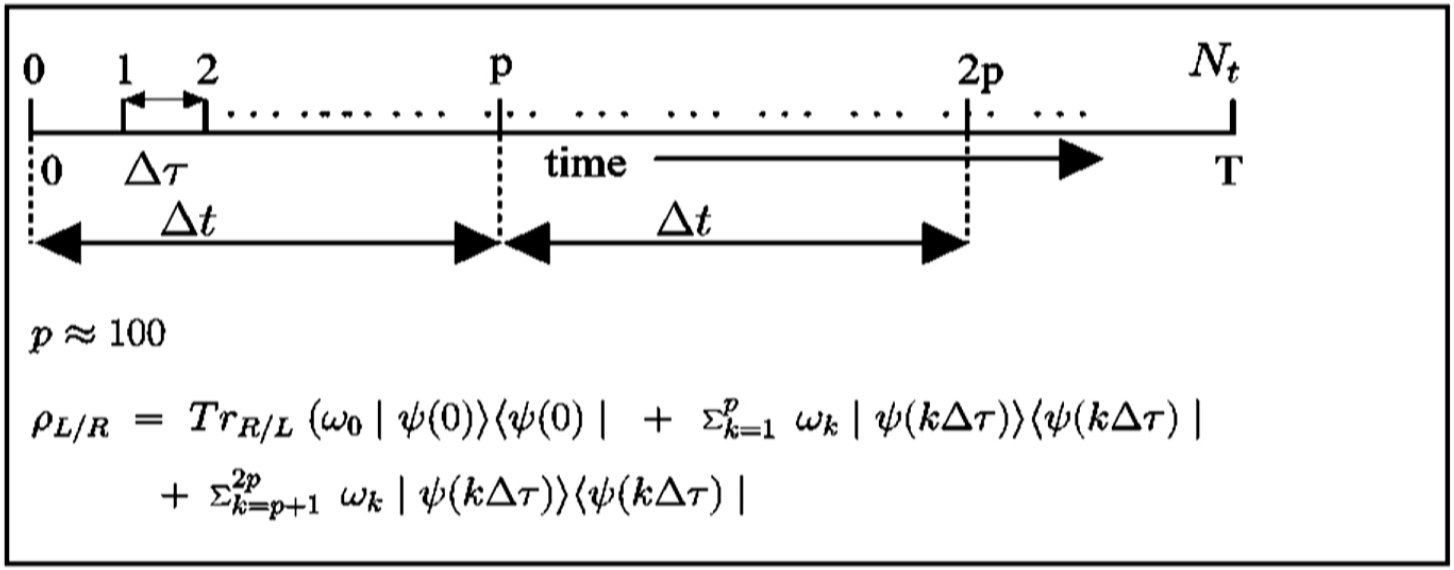

$p \approx 100$

$$\rho_{L/R} = Tr_{R/L}\,(\omega_0 \mid \psi(0)\rangle\langle\psi(0) \mid + \Sigma_{k=1}^{p}\ \omega_k \mid \psi(k\Delta\tau)\rangle\langle\psi(k\Delta\tau) \mid + \Sigma_{k=p+1}^{2p}\ \omega_k \mid \psi(k\Delta\tau)\rangle\langle\psi(k\Delta\tau) \mid$$

Double Time Window Targeting (DTWT) is a hybrid of LXW and TST schemes, which is at least twice as fast and more accurate than either

T. Dutta and SR, Phys. Rev. B, 82, 035115, (2010); Phys. Rev. B 84, 235147 (2011); Phys. Rev., B 85, 035122 (2012).

Charge and spin transport in PPP chains

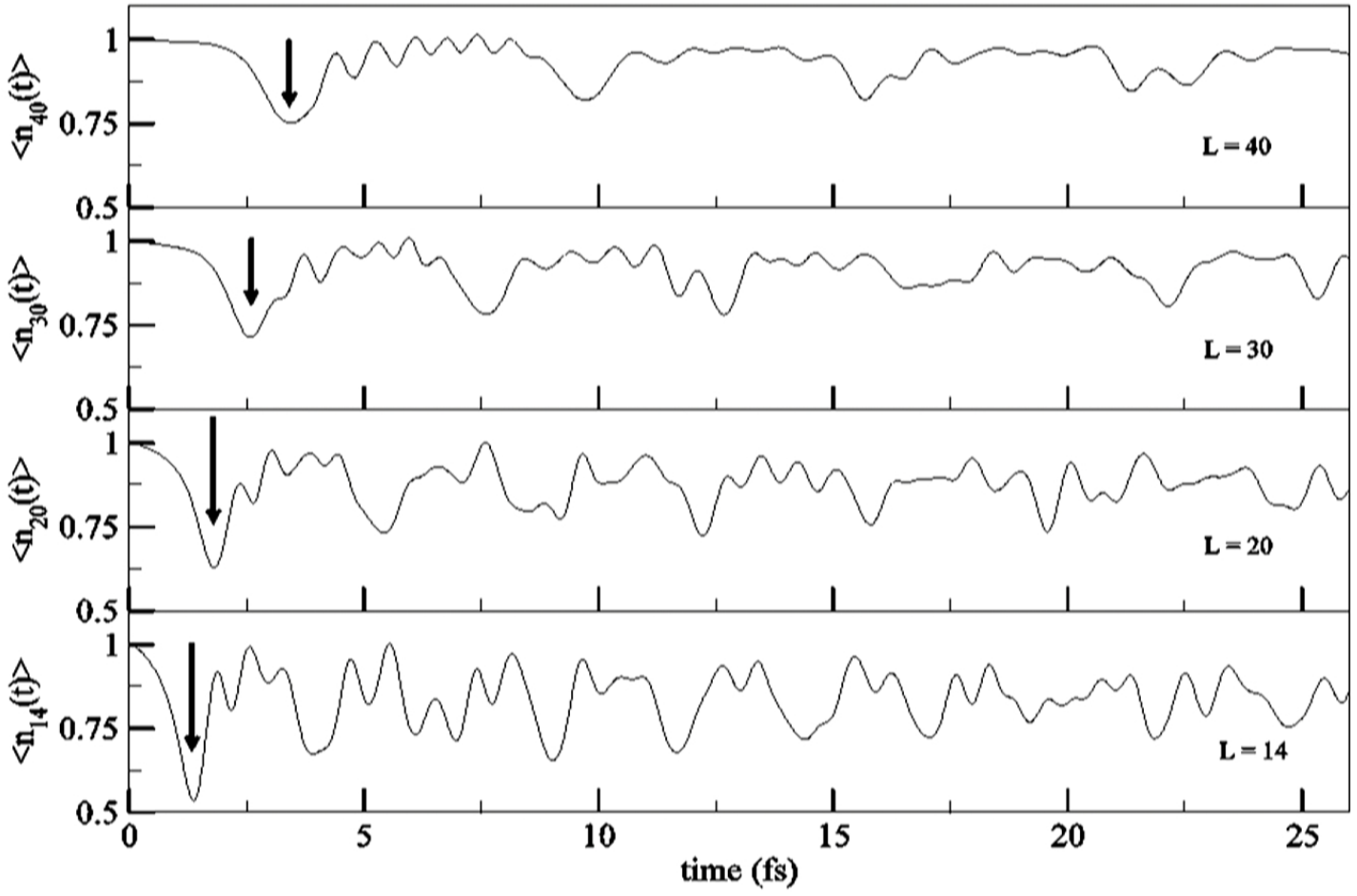

Spin transport in PPP model

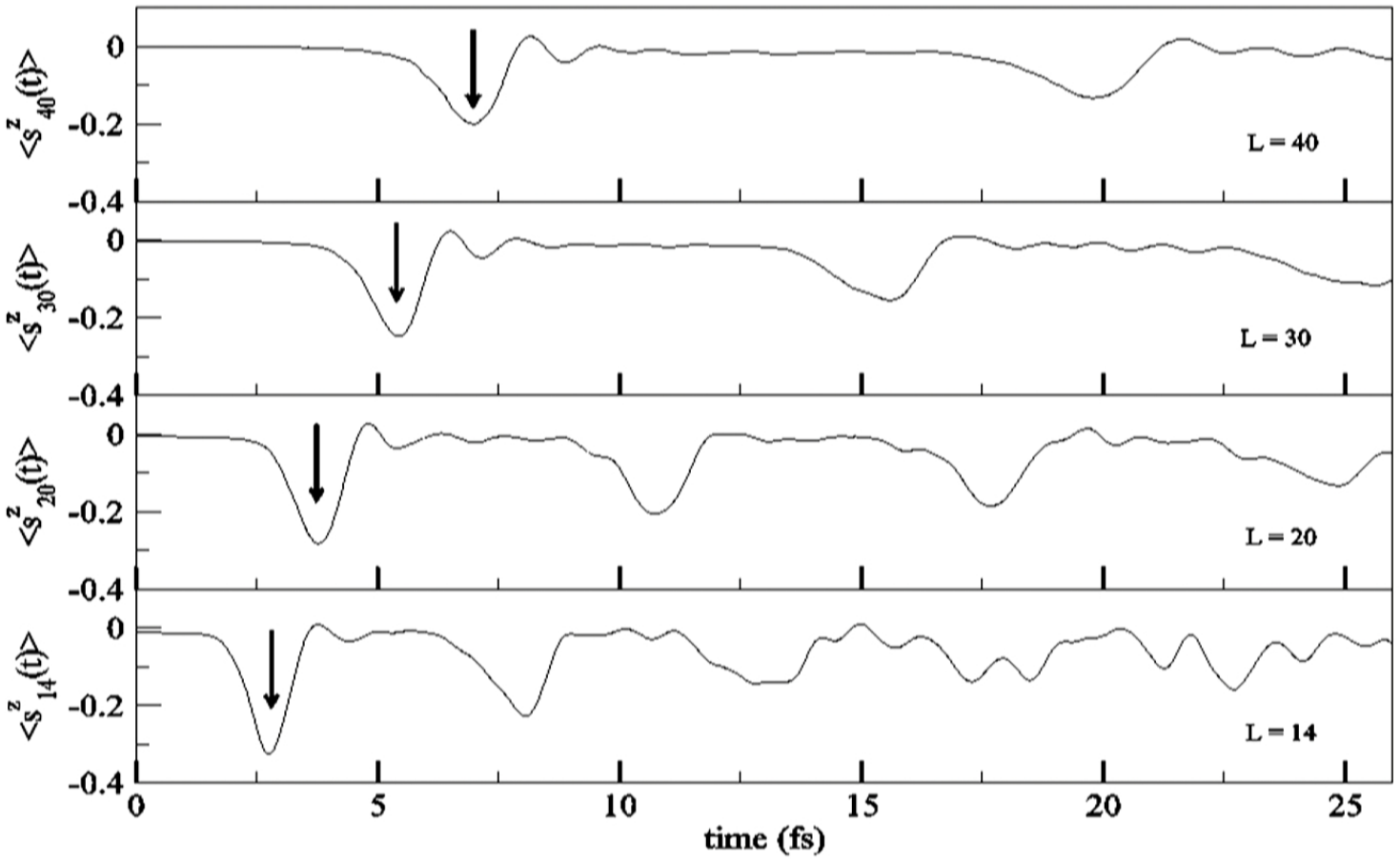

Summary

- Molecular electronic materials based on conjugated organics are strongly correlated systems
- Electron states in these systems are modeled by long range interacting models like the PPP model
- Entanglement entropy of eigenstates of PPP chains are comparable to those of Hubbard models. Hence DMRG method is best suited for solving these models
- DMRG method is extended to target desired excited states, obtain frequency dependent linear and nonlinear responses.
- Efficient real time DMRG algorithm has been developed for wave-packet dynamics.

Thank You